MID-AMERICA TRANSPORTATION CENTER

Report # MATC-KU: 153-4

Final Report

WBS: 25-1121-0005-153-4

Investigation of Driver Adaptations in Mixed Traffic Environment

Alexandra Kondyli, PhD
Associate Professor
Department of Civil, Environmental, and Architectural Engineering
The University of Kansas

Bradley Lane, PhD
Associate Professor
Urban Planning

Saumik Sakib Bin Masud, MSc
PhD Candidate & Graduate Research Assistant
Department of Civil, Environmental, and Architectural Engineering

2024

A Cooperative Research Project sponsored by U.S. Department of Transportation- Office of the Assistant Secretary for Research and Technology

Investigation of Driver Adaptations in a Mixed Traffic Environment

Alexandra Kondyli, PhD.
Associate Professor
Department of Civil, Environmental, and Architectural Engineering,
University of Kansas

Bradley Lane, PhD
Associate Professor
Urban Planning
University of Kansas

Saumik Sakib Bin Masud, M.Sc.
PhD Candidate & Graduate Research Assistant
Department of Civil, Environmental, and Architectural Engineering,
University of Kansas.

A Report on Research Sponsored by

Mid-America Transportation Center

University of Nebraska–Lincoln

August 2024

Technical Report Documentation Page

1. Report No. 25-1121-0005-153-4	2. Government Accession No.	3. Recipient's Catalog No.
4. Title and Subtitle Investigation of Driver Adaptations in a Mixed Traffic Environment		5. Report Date September 2024
		6. Performing Organization Code
7. Author(s) Alexandra Kondyli, PhD, Bradley Lane, PhD Saumik Sakib Bin Masud, MSc., https://orcid.org/0000-0002-5349-2868		8. Performing Organization Report No. 25-1121-0005-153-4
9. Performing Organization Name and Address University of Kansas 1450 Jayhawk Blvd, Lawrence, KS 66045		10. Work Unit No. (TRAIS)
		11. Contract or Grant No. 69A3551747107
12. Sponsoring Agency Name and Address Mid-America Transportation Center Prem S. Paul Research Center at Whittier School 2200 Vine St. Lincoln, NE 68583-0851		13. Type of Report and Period Covered Final Report
		14. Sponsoring Agency Code MATC TRB RiP No. 91994-112
15. Supplementary Notes		

16. Abstract

This study investigates the impact of semi-automated vehicle (SAV) systems, specifically Adaptive Cruise Control (ACC), on driver behavior and control transitions (CT). The variations and adaptations in driver performance due to mental workload, influenced by factors such as task difficulty and driver awareness, are critical, especially under different driving conditions. As ACC systems often fail to provide the necessary deceleration in sudden critical traffic situations, a transition from automated to manual control is triggered. This research aims to predict these CTs using ensemble machine learning (ML) models and to analyze the key factors contributing to these transitions using SHAP analysis. Driving data from 30 participants in both manual and ACC conditions were collected using a driving simulator, including variables such as vehicle trajectories, driver demographics, and mental workload. Various scenarios, including vehicle cut-ins, merging, and lane drops, were developed to capture driver reactions and build predictive models. Among all the ML models, XGBoost produced the best overall performance with accuracy, F1 score, and ROC_AUC values of 0.75, 0.83, and 0.76 respectively. Additionally, SHAP analysis was performed to explore the prominent factors behind the CTs. The study finds significant differences in driving behavior between manual and ACC conditions, with ensemble ML models providing robust predictions of CTs. The findings suggest that age, experience, relative velocity, and perceived mental workload are the key factors behind CT. The results underscore the importance of enhancing ACC systems to improve driver safety and comfort, particularly in critical traffic scenarios.

17. Key Words Adaptive Cruise Control (ACC), Control Transition, Machine Learning, Driving Simulator, Human Factor	18. Distribution Statement		
19. Security Classif. (of this report) Unclassified	20. Security Classif. (of this page) Unclassified	21. No. of Pages 60	22. Price

Table of Contents

Abstract viii
Chapter 1 Introduction 1
Chapter 2 Literature Review 3
2.1 Semi-Automated Vehicles 3
2.1.1 Description and Evaluation of ACC 4
2.1.2 CTs in SAVs 8
2.1.3 Impacts of SAV on Driving Behavior 10
2.2 Car-following Models for Manual Driving 12
2.2.1 Categories of Car-Following Models 12
2.2.1.1 Stimuli-Response Car-following model: GHR Model 12
2.2.1.2 Safety distance category: Gipps model 14
2.2.1.3 Psycho-physical category: Wiedemann model 14
2.2.1.4 Desired measures category: Intelligent Driver Model (IDM) 16
2.2.2 Comparison of car-following models for manual vehicles 18
2.3 Car-following Models for Semi-Automated Driving 21
2.4 Deep Learning-Based Car-following Models 24
2.5 Summary of the Literature Review 27
Chapter 3 Methodology 29
3.1 Prediction Models 29
3.1.1 Bootstrap Aggregating (Bagging) 30
3.1.2 Boosting 30
3.1.2.1 XGBoost 31
3.1.2.2 LightGBM 32
3.2 Inputs and Output 33
3.2.1 Vehicle trajectories: simulator data 33
3.2.2 Driver demographics: survey questionnaires 34
3.2.3 Psychological parameters: eye-tracker data 34
3.3 Performance Metrics 34
Chapter 4 Data Collection 37
4.1 Scenario Development 38
4.1.1 Scenario 1: Base Drive 38
4.1.2 Scenario 2: Vehicle Cut-In 39
4.1.3 Scenario 3: Merging from the On-ramp 39
4.1.4 Scenario 4: Lane Drop 40
4.2 Participants Recruitment 42
Chapter 5 Results and Analysis 43
5.1 Exploratory Data Analysis 43
5.2 Model Performances 49
5.3 Factors Associated with CT 50
Chapter 6 Conclusion and Future Recommendations 52
References 55

List of Figures

Figure 2.1 Wiedemann's car-following model (Wiedemann, 1974) 15
Figure 3.1 Confusion matrix 34
Figure 4.1 KU driving simulator layout (Kummetha et al., 2020) 37
Figure 4.2 Base drive scenario 39
Figure 4.3 Vehicle cut-in scenario 39
Figure 4.4 Merging layout scenario 40
Figure 4.5 Lane drop due to construction scenario 40
Figure 5.1 Boxplot of time headway across different age group 43
Figure 5.2 Boxplot of time headway across different genders (1=Male, 0=Female) 44
Figure 5.3 Relationship of acceleration and brake pedal force with the lead vehicle's velocity.. 45
Figure 5.4 Boxplot of brake pedal forces in ACC and manual driving condition 46
Figure 5.5 Boxplot (a) and kernel density (b) of workload in ACC and manual driving conditions 47
Figure 5.6 CT across different demographics 48
Figure 5.7 Impact of relative velocity and space headway on ACC CT 49
Figure 5.8 SHAP analysis of ACC CT model 50

List of Tables

Table 2.1 Overview of SAE Automation levels 3
Table 2.2 Typical IDM parameters and constraints (Treiber & Kesting, 2013)..... 18
Table 4.1 Summary of driving scenarios for manual driving and semi-automated driving 41
Table 4.2 Summarized data collection..... 41
Table 5.1 Model performances 50

List of Abbreviations (optional)

Mid-America Transportation Center (MATC)
Nebraska Transportation Center (NTC)
Semi-Automated Vehicle (SAV)
Control Transition (CT)
Adaptive Cruise Control (ACC)
Lane Keeping Assistance (LKA)
Machine Learning (ML)
Intelligent Driver Model (IDM)
Workload (WL)

Disclaimer

The contents of this report reflect the views of the authors, who are responsible for the facts and the accuracy of the information presented herein. This document is disseminated in the interest of information exchange. The report is funded, partially or entirely, by a grant from the U.S. Department of Transportation's University Transportation Centers Program. However, the U.S. Government assumes no liability for the contents or use thereof.

Abstract

This study investigates the impact of semi-automated vehicle (SAV) systems, specifically Adaptive Cruise Control (ACC), on driver behavior and control transitions (CT). The variations and adaptations in driver performance due to mental workload, influenced by factors such as task difficulty and driver awareness, are critical, especially under different driving conditions. As ACC systems often fail to provide the necessary deceleration in sudden critical traffic situations, a transition from automated to manual control is triggered. This research aims to predict these CTs using ensemble machine learning (ML) models and to analyze the key factors contributing to these transitions using SHAP analysis. Driving data from 30 participants in both manual and ACC conditions were collected using a driving simulator, including variables such as vehicle trajectories, driver demographics, and mental workload. Various scenarios, including vehicle cut-ins, merging, and lane drops, were developed to capture driver reactions and build predictive models. Among all the ML models, XGBoost produced the best overall performance with accuracy, F1 score, and ROC_AUC values of 0.75, 0.83, and 0.76 respectively. Additionally, SHAP analysis was performed to explore the prominent factors behind the CTs. The study finds significant differences in driving behavior between manual and ACC conditions, with ensemble ML models providing robust predictions of CTs. The findings suggest that age, experience, relative velocity, and perceived mental workload are the key factors behind CT. The results underscore the importance of enhancing ACC systems to improve driver safety and comfort, particularly in critical traffic scenarios.

Chapter 1 Introduction

The ability and performance of drivers can vary greatly between different drivers and even for the same driver in different driving conditions. These variations are influenced by elements such as the driver's mental capacity, the difficulty of the task, perceived risk, and other factors like motivation, exhaustion, drowsiness, drug use, distractions, and stress (Fuller, 2005). The amount of effort a driver needs to make to maintain a steady and safe driving state is called mental workload (Boer, 2001). As task difficulty increases, the mental effort to perform the task increases (Paxion et al., 2014; Silva, 2014).

The Society of Automotive Engineers (SAE International) provides a taxonomy with detailed definitions for six levels of automation (from zero to six): level zero (no driving automation), level one (driver assistance), level two (partial driving automation), level three (conditional driving automation), and level four (full driving automation) (Inagaki & Sheridan, 2019; International, 2018; Teoh, 2020). Nowadays, semi-automated vehicles (SAE levels 2 and 3) co-exist along with manually-driven vehicles. New features like Adaptive Cruise Control (ACC), Automated Lane Following (ALF), and Collision warning systems are equipped in these semi-automated vehicles (SAVs). These new features can provide safe longitudinal or lateral gaps between two successive vehicles. However, the safest maintained distances produced by ACC are typically long enough for surrounding vehicles to cut in. This type of situation requires the SAV driver to take over control of the vehicle.

As the automation level of the vehicle increases, the drivers' mental workload decreases, making them less aware of their surroundings (Ma & Kaber, 2005; Stanton & Young, 2005; Young & Stanton, 2007). Because of that, when a sudden risky event occurs (sudden cut-in or merging), the driver's mental workload increases rapidly in a very short amount of time. As the

driver is less aware, they now have to react quicker (for example, harsh braking) to avoid a collision. This reaction is due to compensating for risky feelings and increased workload, leading to a CT (from semi-automated to manual mode). Braking is one of the most prominent reactions of CT. If the driver did not feel risk and instead felt comfortable during such critical events, they might not press the brake pedal; thus, ACC would not be disengaged. A driving assistant system is unsuccessful if it is not adequately utilized. Thus, it is important to analyze the important factors behind the CT so that necessary steps can be taken in the future to improve the ACC.

Our objective for this research project is to assess car-following behavioral changes of these cognitive parameters due to vehicle automation that may lead to control transitions, and investigate how these changes affect adaptations during car-following.

The specific research objectives are to:

a) Investigate the differences in driving behavior and performance under manual (non-automated) and ACC (semi-automated) driving conditions.
b) Develop a model to predict the control transition in ACC using ensemble Machine Learning (ML) algorithms.
c) Analyze the key factors behind the control transition exploring SHAP analysis.

Chapter 2 Literature Review

2.1 Semi-Automated Vehicles

Driving automation features have been classified into six levels by SAE International (International, 2018; Teoh, 2020). Driver engagement levels along with the various automation features are presented in Table 2.1.

Table 2.1 Overview of SAE Automation levels

SAE level	**Control/ Assistance**	**Features**	**Driver intervention**	**Availability on the present market**
0	No automation control	No automation- manual vehicle	Always	Yes
1	Either lateral or longitudinal assistance	ACC or LKS	Driver has to monitor all the time	Yes
2	Both lateral and longitudinal assistance	ACC and LKS/ALF combined	Driver has to monitor all the time	Yes
3	Both lateral and longitudinal assistance	Features of Level 3 + vehicle takes over responsibility for monitoring the roadway	Driver is expected to be ready to respond only to a request to intervene issued by the driving automation system	Yes (only in Audi A8 vehicle model)
4	Both lateral and longitudinal assistance	Features of Level 3 + vehicle assumes that there will be no driver take over in certain operational design domains	No driver intervention in specially mapped controlled-access roads	No
5	Both lateral and longitudinal assistance	Features of Level 4 + no constrain on operational design domains	No driver intervention at all	No

2.1.1 Description and Evaluation of ACC

The very first term of ACC was Adaptive Intelligent Cruise Control (AICC) which was adopted by the PROMETHEUS program in Europe. The first-generation ACC systems have been on the market since 1995 in Japan, 1998 in Europe, and 2000 in North America (Xiao & Gao, 2010).

With common Electronic Control Units (ECUs) that exist in manually-driven vehicles, one additional slightly modified ECU is added to the ACC system. The additional ECU contains a range sensor and ACC controller which are mounted at the front of the vehicle (Winner et al., 1996). The range sensor is one of the most important components of ACC that collects and transfers information regarding the relative position and speed of two successive vehicles to the control modules (Winner et al., 1996; Xiao & Gao, 2010). There are two types of controllers available in the ACC system: lower-level controller (longitudinal controller) and upper-level (ACC Following controller) (Rajamani, 2012a, 2012b; Rajamani & Zhu, 2002; Xiao & Gao, 2010). If the range sensor does not detect any vehicle in front of it (in the same lane), the longitudinal control dominates and operates like a general cruise control, keeping the vehicle with a constant pre-set-up velocity. The other control is a nonlinear part called the ACC Following controller (Upper-level controller) where the preceding vehicle's information gathered from the range sensor is fed. This control analyzes the information and generates the desired acceleration or deceleration to avoid rear-end collisions. The outputs of the following control systems are the input for the longitudinal control domain.

The longitudinal control has to control and set up the actuators (engine control, transmission control, brake control) to get the desired acceleration calculated by the ACC controller. The ACC system can be deactivated by pressing the switch button or pressing the

brake pedal (Xiao & Gao, 2010). This type of deactivation can be imposed by the driver, whereas in various critical situations ACC automatically deactivates the system by itself. When a required safe deceleration cannot be achieved by the ACC due to some limitations, the system provides notification to the driver to take over.

There are three basic spacing policies for the longitudinal control used in an ACC system: constant distance, constant time headway (CTH), and constant safety factor spacing (Swaroop & Rajagopal, 2001; Xiao & Gao, 2010). To improve the string stability, safety, and reliability, the spacing policies have been updated throughout the years. Xiao et al. mentioned five spacing policies that had been proposed in earlier studies: constant distance, CTH, constant safety factor, constant stability, and constant acceptance. Rajamani et al. showed that strong string stability between the automated vehicles cannot be achieved using the constant distance (space) policy (Rajamani & Zhu, 2002). Recent studies showed that the CTH spacing policy is now applied to ACC systems to improve stability, feasibility, and reliability (Han & Yi, 2006; Zhou & Peng, 2005).

The concerning issues of the ACC system can be categorized into human issues (driver behavior, user-acceptance, human-machine interface), traffic issues (string stability, road capacity, etc.), and social issues (environmental, legal, and marketing issues) (Xiao & Gao, 2010). Through the human-machine interface, drivers can set a time headway and desired velocity for ACC. The limits of these two parameters have been constantly updated throughout the years. According to Winner et al., the upper limit of the time constant (set-up gap) should not exceed 2 s, and values around 1 s are reasonable (Winner et al., 1996). The study also explored that the ACC system lacks the capability of emergency braking, and the maximum acceleration and deceleration rates were considered as 2.5 m/s^2 and 1 m/s^2 respectively for smooth braking.

This was one of the biggest limitations of ACC vehicles as with these values the vehicle cannot brake on time in emergency and critical traffic conditions. The study also investigated the limitations of ACC vehicles due to geometric obstruction and weather conditions (Winner et al., 1996). In acute weather conditions (heavy rain or snow) the sensors could get jammed and ACC could fail to operate.

Larger time gaps of ACC-equipped cars can decrease traffic flow. Winner et al. showed that at a 20% penetration rate of ACC vehicles, the decrease in traffic flow was noticeable (Winner et al., 1996). Thus, further research works have been focusing on developing algorithms that can generate smaller gaps (for ACC equipped vehicles) to increase string stability. Generally, commercial ACC systems are designed with a CTH spacing policy that produces a time gap between 1 and 2 s. This gap is large enough for a manual or automated vehicle to cut in and it can cause string instability. Rajamani et al. investigated the upper-level controller and created a new design of the controller for ACC that determines the acceleration based on its own speed, headway, and relative speed from the preceding vehicle in the same lane on a highway (Rajamani & Zhu, 2002). The design especially considers optimizing string stability between successive vehicles in the same lane. The proposed system is called the Semi-autonomous ACC (SACC) which combines the advantages of typical ACC systems with the performance and traffic flow advantages of a platoon system. In this system, if a SACC vehicle detects another SACC vehicle in front of it, it will close the gap to a few meters, taking advantage of the smoother and safer ride of the SACC system. If the detected preceding vehicle is manual, the SACC would work like a traditional ACC producing larger inter-vehicular spacing. The paper analytically shows that by being able to maintain smaller (and safer) time gaps the proposed

system was able to improve string stability and provide smoother performance than the standard ACC system.

Kesting et al. proposed an extended ACC system where the updated ACC adapts the driving style based on different traffic conditions (Kesting et al., 2007). The system produced acceleration/deceleration as a function of not only preset velocity and headway but also traffic flow. A traffic state detection model was developed that utilized the vehicle's own velocity and the exponential moving average (EMA) method to detect five different traffic conditions: free traffic, approaching congestion (upstream front), congested traffic, leaving congestion (downstream front), and infrastructural bottleneck sections. The study incorporated the traffic state detection model into the car following model to calculate the acceleration rate. The proposed model showed that with a small penetration rate (25%) of the proposed ACC system, the travel time was reduced by improving the traffic stability and flow to a great extent.

Davis (2004) showed the effects of the ACC system on traffic flow by simulating different penetration rates of ACC in various traffic scenarios (on-ramp, single lane, and multilane highways) (Davis, 2004). The ACC vehicles were modeled by linear dynamic equations that had string stability. At high speeds (around 30 m/s) traffic jams decreased while the penetration rate of ACC was greater than 10% and the jam disappeared at a 20% penetration rate. The occurrence of jams also depended on the sequence of the ACC and manual vehicles. The case was different in moderate traffic flow (around 15 m/s) where the increase in the penetration rate of ACC did not prevent jamming but increased the overall speed in the queue discharge region. A small improvement in traffic flow was seen at a random 50% penetration rate of ACC on a multilane highway. Short time headway of ACC increased the throughput although the average velocity in the shoulder lane at the entry of merging decreased because the

ACC system does not give proper space to the on-ramp vehicles for safe merging like the manual vehicles can (depending on driver behavior). To improve safety, video cameras and thermal radiation sensors are being added to some ACC systems available in the market (Jurgen, 2006; Xiao & Gao, 2010).

2.1.2 CTs in SAVs

A driver can take over and disengage the automated systems in semi-automated vehicles by performing different reactions. For instance, braking will disengage the ACC. Transitioning from automated mode to manual mode (and vice versa) is called CT.

Varotto et al. formulated a decision-making model to estimate the feeling of risk using the Risk Allostasis Theory (RAT) (Varotto et al., 2018), which was further utilized to forecast driver's reaction and response to the driving assistance system and adapt its settings to prevent CT. Thus, this model improved safety and comfort. However, this generic framework did not include congestion level, presence of vehicles in nearby lanes, percentages of heavy vehicles, number of lanes including the physiological parameters such as workload, heart rate, etc., as its explanatory variables.

The transition period refers to the time needed to adapt and stabilize driving behavior after disengaging (Varotto et al., 2020). Therefore, exploring how these systems affect driver behavior is necessary to determine the factors of disengaging the ACC. Varotto et al. investigated in which situations CTs occur, by analyzing the velocity, acceleration, and headway of the subject and front vehicle and how these dynamic parameters change within the CT (Varotto et al., 2014). The study also focused on the types of participants that tend to transition more from automated to manual mode. They found that gender and experience with the new systems have significant correlation with the disengagement of ACC. In a follow-up study,

Varatto et al. found that traffic density also affects the CT behaviors of drivers (Varotto et al., 2020).

Calvi et al. analyzed driver behavior after a CT. According to the study, the driving experience with automated systems has an impact on transition behavior (Calvi et al., 2020). The main focus of this research was to assess the effects of an automation period on drivers in terms of driving performance (speed, acceleration, headway) and safety (TTC). The study revealed that drivers could maintain driving with ACC if the system's decrease in velocity and deceleration produces less risk and higher comfort. This finding is consistent with a study that showed that drivers most likely do not resume ACC after deactivating it, especially in dense conditions (Varotto et al., 2017), when ACC does not produce appropriate velocity and deceleration to decrease the feeling of risk and improve comfort.

A recent study correlated reaction time with take-over request (TOR) by analyzing eye movements (Y. Wu et al., 2021). A total of 36 participants drove SAE level 2 vehicles on a road and a cone was placed on the road at the end of the study which was the critical TOR event for the study. The inside camera of the vehicle captured the eye movement measurements: percentage of front fixation, size, and velocity of the saccadic eye movements. They calculated the reaction time in terms of both steering and braking behavior. The reaction time for the steering operation was defined as the time consumed after TOR until the steering angle became 1.5 degrees from 0 degrees. The reaction time for the braking was defined as the time consumed after TOR until the brake pedal was pressed at 1% of the full braking. The smaller of these two reaction times was considered as the reaction time to TOR in critical events. The study revealed that the reaction time to TOR was found to be longer when there was a smaller number of large saccades, a greater number of medium saccades, and lower saccadic velocity.

2.1.3 Impacts of SAV on Driving Behavior

Stanton et al. investigated the effects of ACC on driving psychology (Stanton & Young, 2005). The study revealed that drivers feel they have less control while driving with ACC-equipped vehicles; which makes them reduce their trust in automation. In that study, participants drove both in manual and ACC mode in various levels of traffic flow (low, medium, and high) in a driving simulator environment. The authors analyzed variance (ANOVA) to measure the effect of ACC on workload, situation awareness, trust, stress, and locus of control. The overall workload was found to be lower in manual driving conditions than in ACC conditions and it changes with the change in traffic. Although while driving with ACC the workload was found to be higher in medium traffic than in lower traffic, the workload was again lower in higher traffic conditions. The study suggested that a properly updated ACC can be most useful in high-traffic conditions. The level of frustration increased while driving lower traffic to medium traffic with the manual vehicle. When driving with ACC the frustration decreased with a slight increment in traffic (lower to medium). In high-traffic conditions, the frustration level was higher in ACC than in manual vehicles. The study suggested that the optimum design of ACC will be able to reduce workload in medium and high-density traffic without reducing the situation awareness of the drivers.

Drivers reduce their level of attention while driving with ACC. Automation systems generally decrease the perceived workload from the environment, making drivers inattentive. Paradoxically, while approaching complex highly-dense traffic, inattentive drivers have to go through a higher cognitive load (Stanton et al., 1997; Stapel et al., 2019). Stapel et al. quantified subjective workload (perceived) and objective workload (cognitive load) through NASA R-TLX and Detection Response Time (DRT) respectfully for both manual and semi-automated driving

(Stapel et al., 2019). They conducted the experiment on the road and found that increased traffic complexity increased both workloads. Driver's experience in automated driving had an impact on the perceived workload. Automation-experienced drivers faced less subjective workload than inexperienced drivers while driving in an automated environment. Although the perceived workload was found to be lower for automation-experienced drivers, the cognitive load (objective workload) was high for both experienced and inexperienced drivers in automated driving mode. The increased complexity of the traffic scenario had a similar impact on manual and automated driving. The workload did not decrease in an automated environment in such conditions.

Manawadu et al. classified drivers' perceived workload associated with five different levels of traffic complexity (Manawadu et al., 2018). They used driver psychological signals (electrocardiography, electrodermal activity, and electroencephalography) and subjective workload measurements to classify driver perceived workload utilizing a memory-based recurrent neural network (LSTM). Biondi et al. evaluated the effects of semi-automated driving in real life in terms of physiological and behavioral measurements, and compared them with manual driving (Biondi et al., 2018). The levels of driver arousal were found to be lower during semi-automated driving. They concluded that semi-automated driving decreases situation awareness and increases cognitive load as the detection response time becomes slower. These findings align with previous studies (De Winter et al., 2014; Stapel et al., 2019), although the study was performed by automation-inexperienced drivers only.

Miller et al. evaluated the longitudinal and lateral effects (behavioral adaptation) of ALF in terms of TTC and standard deviation of lateral position (SDLP) respectively (Miller & Boyle, 2019). The study was performed through a driving simulator where participants drove in both

manual and semi-automated modes. DRT was also measured in various traffic conditions to check the awareness and engagement of the drivers. Repeated measures of ANOVA showed that ALF decreased the SDLP and average TTC of the drivers. But the lateral deviation increased just after disengaging the ALF system. While driving with ALF, after a certain period when the ALF was disengaged by the driver, the SDLP increased to a certain value that was greater than the value collected from manual driving conditions. Drivers' mean TTC was much lower when the ALF was activated compared to their own mean TTC when driving manually. The reduction in mean TTC continued even after disengaging the ALF. It was suggested that the lateral assistance system also has an impact on longitudinal driving behavior. The cognitive workload decreased driving with the ALF system, which led the drivers to over-trust these lateral assistance systems and start performing secondary tasks. The study showed that attention to the secondary tasks increased when the ALF was turned on.

2.2 Car-following Models for Manual Driving

2.2.1 Categories of Car-Following Models

2.2.1.1 Stimuli-Response Car-following model: GHR Model

To characterize car-following behavior in a variety of situations, many mathematical models have been constructed. Most of the models were developed by adopting a stimulus-response framework. The stimulus-response framework was developed in the General Motors research laboratory by Chandler et al., (1958) and Gazis et al. (1961). The framework assumes the driver's response to a given situation maintains the following relationship:

$$response = sensitivity * stimulus \quad (2.1)$$

Using the stimuli-response framework, Chandler et al. (1958) and Herman et al. (1959) developed the first linear car-following model as shown in Equation 2.2:

$$a_n(t) = \lambda . \Delta Vn(t - \tau_n) \quad (2.2)$$

Where: $a_n(t)$ is the acceleration of the n^{th} subject vehicle at time t, $\Delta V_n(t-\tau_n)$ is the velocity difference between the subject and preceding vehicles at time t, τ_n is the reaction time of the n^{th} vehicle's driver, and λ is the sensitivity parameter which can be constant or a step function.

Many researchers developed their own equation to describe λ in various aspects of car-following behaviors. Gazis et al. combined the constant and stepwise function of λ to update the linear car-following model to a non-linear car-following model, shown in equation 2.3.

$$a_n(t) = \boldsymbol{\alpha} V_n(t)^{\beta} \frac{1\Delta V_n(t-\tau_n)}{\Delta X_n(t-\tau_n)^{\gamma}} \quad (2.3)$$

Where: a, β, γ are parameters.

The GHR model has been widely used since it was introduced to model car-following behaviors because of its simplicity. However, the model was developed considering some assumptions that might not apply to real-world scenarios. For example, the reaction time was assumed to be constant and identical for all the drivers which is not realistic. The model also overestimated the driver's capability to perceive small changes in relative velocity and headway.

2.2.1.2 Safety distance category: Gipps model

In contrast to GHR models, safety distance models contend that the driver responds to spacing relative to the previous vehicle rather than to relative speed (Saifuzzaman & Zheng, 2014). These models are also called collision-avoidance models and the basic idea of these models was developed by Kometani & Sasaki (1959). Later, Newell updated the models to adopt a non-linear effect in the car-following dynamics (Newell, 1961). Newell assumed the velocity of the subject vehicle was a non-linear function of the relative distance (gap) between the subject and the preceding vehicle. The most used and popular car-following model in this category is the Gipps' car-following model. Gipps' model assumed that drivers select the velocity of the vehicle in such a way that, if the preceding vehicle suddenly presses the brake or stops, the subject vehicle will be able to stop without colliding with the preceding vehicle (Gipps, 1981). Gipps provided two separate equations of velocity for free flow and car-following conditions, where the driver chooses the minimum of these two velocities while driving. In this model, the reaction time was set to be constant. The transition from the free flow state to the car-following state was found to be smoother but not in some critical conditions like the hard brake of the preceding vehicle, or vehicle cut in between two successive vehicles. This model also provided some behavioral parameters like desired velocity and acceleration, reaction time, and the deceleration rate of the preceding vehicle.

2.2.1.3 Psycho-physical category: Wiedemann model

Drivers cannot perceive small changes in spacing and relative velocity. Therefore, thresholds for spacing and the relative velocity between the following and preceding vehicles have been defined in certain categorical car-following models, called the psycho-physical models. The Wiedemann is the most popular psycho-physical car-following model developed,

where Wiedemann defined the threshold value of the stimulus that a driver can perceive and react to, and named it the "perceptual threshold" (Wiedemann, 1974). The drivers are able to change their behavior (by reacting) when the perceptual thresholds are reached (Leutzbach, 1988).

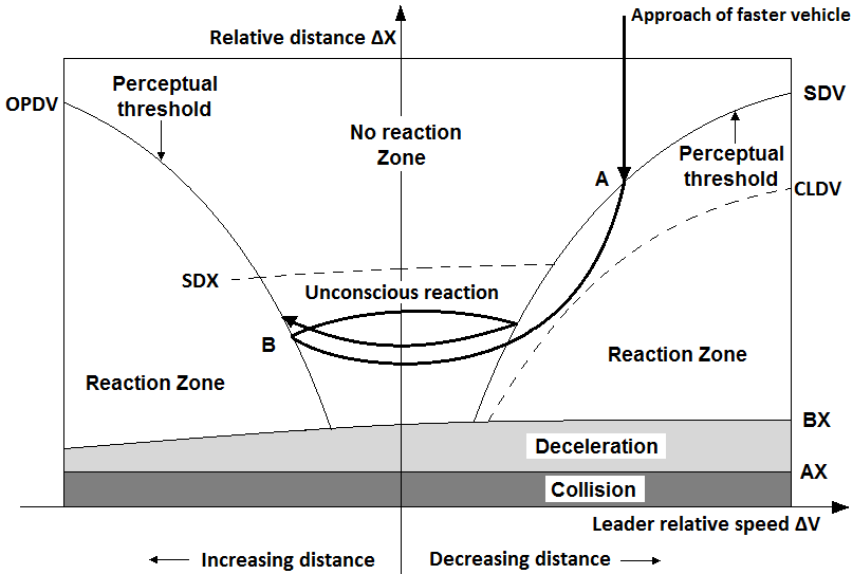

Figure 2.1 Wiedemann's car-following model (Wiedemann, 1974)

In Figure 2.1 the Wiedemann model considers six perceptual thresholds:

- the desired space headway of two standstill successive vehicles (AX);
- the desired minimum headway which is a function of AX, velocity, and safety distance (BX);
- a point when the driver understands that they are driving at a higher velocity than the lead vehicle (SDV);
- the additional threshold for additional deceleration to apply the brake when the lead vehicle is slower than the following vehicle (CLDV);

- the action point when the driver realizes that the speed of the following vehicle is lower than the preceding vehicle's speed, and starts to accelerate (OPDV); and
- the perception threshold to model the maximum following distance (SDX) (Saifuzzaman & Zheng, 2014).

From Figure 2.1, the dark line refers to the decision path of the following vehicle. When a vehicle is traveling faster than the leader, the vehicle will be getting closer to the leader until the deceleration perceptual threshold (SDV) point is reached (Point A). The driver will then apply the brake to decelerate until they match the velocity of the lead vehicle. As human beings are unable to track the small changes in relative velocity, the spacing between the vehicles will increase until the acceleration perceptual threshold (OPDV) is reached at Point B. After reaching Point B, the driver will understand that the following velocity is lower than the preceding vehicle's velocity and apply acceleration to again match the lead vehicle's speed. This process is continuous, as shown in the "unconscious reaction zone" in Figure 2.1.

By Wiedemann's suggestion, a slightly modified version of the Wiedemann model has been incorporated into the commercial microsimulation software VISSIM (Fellendorf & Vortisch, 2010). Since then the model (VISSIM) is being constantly updated.

2.2.1.4 Desired measures category: Intelligent Driver Model (IDM)

Car-following models that consider desired measurements, such as desired velocity or desired headways, fall under this category. Several desired-measure categorical car-following models have been developed by Helly (1959), Koshi et al. (1992), Xing et al. (1995), Treiber et al. (2000) among others. Among them, the IDM is the most popular and most used car-following model because of its simplicity. The IDM was proposed by Treiber et al. where they considered

both desired speed and desired space headway to develop the model (equations 2.4 and 2.5) (Treiber et al., 2000).

$$a_n(t) = a_{max}^{(n)} \left[1 - \left(\frac{V_n(t)}{\tilde{V}_n(t)}\right)^{\beta} - \left(\frac{\tilde{S}_n(t)}{S_n(t)}\right)^2\right] \tag{2.4}$$

$$\tilde{S}_n(t) = S_{jam}^{(n)} + S_1^{(n)}\sqrt{\frac{V_n(t)}{\tilde{V}_n(t)}} + V_n(t)\tilde{T}_n(t) - \frac{V_n(t)\Delta V_n(t)}{2\sqrt{a_{max}^{(n)} b_{comf}^{(n)}}} \tag{2.5}$$

Where, $a_n(t)$ is the acceleration of the subject vehicle n at time t, $a_{max}^{(n)}$ is the maximum acceleration of the subject vehicle n, $V_n(t)$ is the actual speed of the subject vehicle n at time t, $\tilde{V}_n(t)$ is the desired speed, $S_n(t)$ is the spacing between two successive vehicles at time t (front of the follower to rear of the leader), $\tilde{S}_n(t)$ is the desired minimum gap between two successive vehicles, $S_{jam}^{(n)}$ is the minimum spacing at standstill, $\Delta V_n(t)$is the relative velocity at time t, $\tilde{T}_n(t)$ is the desired time headway, $b_{comf}^{(n)}$ is the comfortable deceleration, and β is a parameter that characterizes how acceleration decreases with speed.

The IDM is the combination of the free-flow and car-following model that considers both the desired speed and the desired space headway (Saifuzzaman & Zheng, 2014). The desired space headway is a function of the subject vehicle's speed, relative velocity, minimum spacing, maximum acceleration, and comfortable deceleration. Although the transition between the free-flow and car-following model is smooth, the model does not consider reaction time. Various studies have calibrated this model for various purposes. For example, Treiber and Kestin calibrated the IDM and established typical values for city and highway driving (Treiber &

Kesting, 2013). According to their research, the typical IDM parameter values are stated in Table 2.2.

Table 2.2 Typical IDM parameters and constraints (Treiber & Kesting, 2013)

Parameters	**City values**	**Highway values**	**Constraints**
desired speed, $\tilde{V}_n(t)$	15.0 m/s	33.3 m/s	1 to 70 m/s
Time headway, $\tilde{T}_n(t)$	1.0 s	1.0 s	0.1 to 5 s
Minimum spacing, $S_{jam}^{(n)}$	2 m	3 m	0.1 to 8 m
Acceleration component, β	4	4	1 to ∞
Maximum acceleration, $a_{max}^{(n)}$	1.0 m/s2	1.0 m/s3	0.1 to 6 m/s2
Comfortable deceleration, $b_{comf}^{(n)}$	1.5 m/s2	1.5 m/s3	0.1 to 6 m/s2

2.2.2 Comparison of car-following models for manual vehicles

Sangster et al. used a naturalistic dataset to calibrate four car-following models and compared the model performances (Sangster et al., 2013). The study calibrated the Gipps, the IDM, the GHR, and the Rakha-Pasumarthy-Adjerid (RPA) models. Among them, the RPA model performed the best, followed by the Gipps model. Though the RPA and Gipps models provided less variability in behavior compared to the IDM and GHR models, the IDM and GHR models were seen to fluctuate significantly compared to the real observed data.

Zhu et al. calibrated and validated five car-following models (GHR, Gipps, IDM, Full Velocity Difference, and Wiedemann) on naturalistic data collected from an urban expressway in Shanghai, China (Zhu et al., 2018). The authors randomly selected 42 drivers whose ages ranged

from 25 to 60, their driving experience ranged from 1 to 23 years, and 20% of the drivers were females. Only car-following data were extracted from the naturalistic database for modeling purposes. The sensors for obtaining relative velocity, acceleration, and spacing were equipped in the vehicle. Besides the trajectories, each vehicle captured the driver's face, forward roadway, roadway behind the vehicle, and hand movement of the driver through four video cameras. The study adopted a Genetic Algorithm (in MATLAB) to find the optimum values for the car-following model parameters. Root Mean Squared Percentage Error (RMSPE) was used to evaluate the models. The results showed that the IDM performed the best among the remaining models with the lowest RMSPE value. The GHR and FVD models had low calibration errors and high validation errors, which made these models unreliable. The IDM also showed the lowest standard deviation among the vehicles, which made this model stable and reliable. In the validation phase, the GHR and FVD had the highest number of collisions (40 and 50 respectively) whereas the Wiedemann model had only 4, and IDM did not produce any collision.

In a car-following situation, the trajectory and the driver's behavior mostly depend on the type of front vehicle. Wu et al. proposed a preceding vehicle type-based car-following model using naturalistic data (Wu et al., 2019). They analyzed one and half years of naturalistic data by multivariable Gaussian Mixture model (GMM) to establish that driver's following behavior depends on the type of the preceding vehicle. A Hidden Markov model (HMM) was developed to detect the type of front vehicle (for both steady and dynamic conditions) whether the vehicle is a car, bus, or truck. The study used radars and cameras to get the real-time vehicle velocity, relative velocity, relative distance, engine speed, acceleration, gear position, brake pressure, and steering wheel angle from 16 vehicles. Taking the preceding vehicle's type into the consideration, they proposed a new car-following model for each of the leading vehicle types

where the velocity and relative distance of the vehicle were predicted. They compared the proposed model with other car-following models such as Cellular Automata (CA) and IDM, using RMSE and RMSPE as performance metrics, and showed that the proposed model can mimic the natural driving behavior of the driver better than any of the stated models. The RMSE values for relative distance prediction by the proposed model were 0.07 m, 0.08 m, and 0.22 m for car, bus, and truck respectively; whereas IDM produced the RMSE values of 0.42 m, 0.50 m, 4.44 m and CA produced RMSE values of 1.35 m, 2.35 m, 14.52 m. The authors declared that the proposed car-following model is suitable for the condition with a changing lead vehicle type.

Zhang et al. compared four different types of car-following models using large-scale naturalistic driving data from Shanghai (Zhang et al., 2021). The study adopted four models: the GHR model (stimuli-response category), Gipps model (safety distance category), the Intelligent Driver Model (IDM) (desired measures category), and Wiedemann model (psycho-physical category). The data included 50 drivers and captured both uninterrupted flow and interrupted flow facilities. The Root-Mean-Square Normalized Error (RMSNE) of the relative spacing was used for the performance evaluation of the models. The two-sampled Kolmogorov-Smirnov (K-S) test showed that the error distribution of the four models was significantly different from each other. The results showed that the Gipps model produced the highest number of collisions, the GHR model produced the highest error, and IDM provided the best overall performance with an RMSNE of 0.05. The standard deviation and cumulative density function (CDF) were used to compare the model stability. The IDM produced the best results in terms of stability, whereas, the Gipps model showed the highest standard deviation (instability). The participating drivers were divided into three groups with three different driving styles: timid, neutral, and aggressive. The four car-following models were calibrated for each driving style to see which model works

better for a specific style of driving. For all three types of driving styles, the IDM outperformed all the other models in terms of accuracy and stability. Although the average error of the Wiedemann model on timid and neutral styles was found higher than the Gipps model, the stability of the Wiedemann model was better than the Gipps model. The average calibration error increased with the aggressiveness level for all models.

2.3 Car-following Models for Semi-Automated Driving

A few studies have recently investigated the car-following behavior of the ACC. Different studies developed their car-following models focusing on different aspects of driving (efficiency, safety, fuel economy, or comfort). Yang et al. developed a car-following behavior model for a sag section of the road to improve the ACC system (Yang et al., 2015). The model was developed based on Helly's car-following model where they computed the required acceleration and reaction time while driving an ACC-equipped commercial vehicle on a sag road segment. The study borrowed the concept of the effect of sag segments on car-following from research by Oguchi (Oguchi, 2009) that updated Helly's model. Yang et al. used RMSE as a performance indicator to compare the proposed model with Helly's original model (Yang et al., 2015). The model was calibrated with a field-observed dataset to obtain the model parameters. The study found that 48.9% of the drivers (driving with ACC) were affected by the vertical slope which Helly's original model failed to capture. Analyzing the performance of the model on both manually-driven and ACC-equipped vehicles they concluded that 28.8% of the manually-driven vehicles outperformed the ACC systems in reacting to perturbation. They suggested designing ACC algorithms based on a specific road segment like a sag section that would improve the efficiency of maintaining comfort and safety.

Improving fuel consumption and comfort level can increase the usage of ACC in commercial vehicles. Luo et al. proposed an algorithm for ACC based on a predictive control framework for multiple objectives (Luo et al., 2010). The proposed ACC system measured the current inter-spacing, own velocity, relative velocity, acceleration, and jerk. The algorithm not only satisfied the car-following behavior ensuring safety but also improved fuel economy with comfortable driving. To evaluate the performance of the proposed model they developed two ACC algorithms: one where they considered comfort, fuel economy, safety, and car-following (ACC_CFSC), and one that considered only safety and car-following (ACC_SC). Vehicle cut-in, cut-out, and hard/sudden braking events were included in the simulated traffic scenarios. The results showed that both ACC_CFSC and ACC_SC guaranteed safety by modeling car-following behavior with no collision. The regulated speed and adjusted headway were in accord with the safe car-following behavior. The comfort in driving was measured by the values of acceleration and jerk. The comfort driving indicated the lower values of acceleration and jerk. The simulation results showed higher comfort in vehicles equipped with ACC_CFSC rather than ACC_SC. For instance, in the scenario of approaching a stationary vehicle, the acceleration and jerk reductions were 41.4% and 74.2% respectively which indicated an improvement in driving comfort. In terms of evaluating the fuel consumption based on the smoothness of the responses, the ACC_CFSC was smoother. For instance, in the cut-out scenario, the ACC_CFSC and ACC_SC both maintained similar gaps, velocity, and acceleration, but smaller fluctuations (smoother graph line) were found in ACC_CFSC. It was indicated that both algorithms worked well in terms of safety aspects but ACC_CFSC had the privilege of a smoother ride which provided more comfort and less fuel consumption.

Xiao et al. developed a collision-free car-following model for ACC/CACC vehicles using vehicle trajectories (Xiao et al., 2017). The developed model assumed that a driver takes back control of the vehicle in two situations: i) depending on the judgment of the driver or ii) getting a take-over request from a collision warning system. According to the study, the drivers are assumed to take over from ACC while approaching a slow-moving vehicle with a relative speed of 15 mph. Driver's perception to detect and act with the low-speed leader was found to be the root of the override time. The model inputs were the speed and position of the subject and preceding vehicles along with the desired set-up cruise velocity and time gap of the drivers (which was set using the ACC system). The model output the desired acceleration that would eliminate collisions to provide a safer ride. Several traffic scenarios were created in MATLAB which included stop-and-go, hard brake, cut-in, cut-out, and approaching scenarios. Under these scenarios, the developed model showed good results in terms of collision-free string operation. The proposed model did not cause any collision in either long-lasting soft braking or hard braking situations in the microsimulation.

Yu et al. explored the impact of a memory-based relative velocity difference (RVD) strategy on vehicular trajectories and fuel economy in ACC-equipped vehicles (Yu et al., 2018). They simulated a car-following model with this strategy and included the driver's delay time (or reaction time of the controller) as an input with relative velocity, the following vehicle's velocity, and the vehicular gap. The model's goal was to reduce the deviation between the simulated headway and the simulated headway of two subsequent vehicles. The RVD model had different memory steps with different effects on the standard deviation of the vehicle speed. It was found that the standard deviation of a vehicle initially decreased and gradually increased with the increment of the memory steps. The study suggested that a memory-based CF model

can improve the overall stability and comfort by accelerating or decelerating much earlier, and the effective memory interval was found to be two seconds to seven seconds. The model verified that considering RVD with memory significantly improves the overall stability, comfort, and fuel economy of ACC.

2.4 Deep Learning-Based Car-following Models

Artificial Intelligence reflects the natural evolution of technology as increased computing power enables computers to sort through large datasets to identify patterns and predict more accurately and time efficiently. Car-following models using Deep Learning (DL) are able to capture the asymmetric driving-behavior in various types of driving situations with higher accuracy. Embedding a long memory into car-following models can improve the model prediction as it can consider the long-term relationship between acceleration, velocity, spacing, and relative velocity. There are a few memory-based deep learning methods currently available, e.g., Long Short-Term Memory (LSTM), Gated Recurrent Unit (GRU), etc., that are reliable predictors.

Wang et al. implemented a deep learning algorithm (GRU) based car-following model using historical data (Wang et al., 2017). GRU is a similar kind of deep neural network as LSTM that can store memory. In that study, they used the US 101 highway dataset (from 7:50 AM to 8:35 AM) from NGSIM (*NGSIM*, 2016) to build the model and showed that using 10 seconds of historical inputs produced the best accuracy. The GRU model consisted of three hidden layers with 30, 10, and 10 neurons in each layer, respectively. Though one step prediction produced by GRU outperformed other models (Feed-forwarded Neural Network (FNN), IDM, LSTM), the models lacked some useful information such as vehicle type, headways, and lane conditions.

Huang et al. developed a data-driven car-following model considering driver asymmetric behavior using LSTM (Huang et al., 2018). The NGSIM data (*NGSIM*, 2016) were utilized for model training and validation. The input variables of the model were the historical information of the velocity of the subject vehicle, velocity difference with the lead vehicle, and the gap between the two vehicles (rear to front bumper). The LSTM model was trained and calibrated with this historical information (input variables) to predict the velocity of the subject vehicle in the next time step. The LSTM model required several parameters to be tuned perfectly for the specific dataset to improve the accuracy and reliability of the model. They adopted the optimal historical time step and number of training data by trial and error, and 5 s of the historical time produced the highest accuracy. To compare the performance and overall reliability of the model, they compared the proposed LSTM model with other deep learning models, namely the Recurrent Neural Network-based CF model (RNN) and the Asymmetric Full Velocity Difference model (AFVD). The LSTM outperformed the other models by achieving the lowest MSE and R values on both the training and testing datasets. While predicting velocity, the RNN performed the worst among the models with a much higher testing error showing poor reliability. All the errors of the LSTM model were found to be lower than the other models. The lowest standard deviation of the LSTM prediction indicated the stability of the model compared to RNN and AFVD models.

Wu et al. developed a car-following model called Memory, Attention, and Prediction (MAP) that consisted of two deep learning sub-models called the prediction model and action model (Wu et al., 2019). Both models were generated by a GRU. The model inputs were the velocity, headway, and acceleration of the following and lead vehicles. Before building the models, an attention mechanism was used to select the most relevant information, filtering out

the irrelevant information and variables (e.g. acceleration of lead vehicle). The acceleration of the following vehicle was the output of the prediction model whereas, in the action model, the following vehicle's velocity and movement distance were considered as the outputs. A part of the US Highway 101 dataset from NGSIM (*NGSIM*, 2016) was used for the model training and validation. Only 15 minutes of data (20,000 samples of the first three lanes) were used for training where the historical length was set to be 10 steps, which means one-second historical trajectories were used as inputs. Comparing the developed model (MAP) with other deep learning models and IDM they concluded that MAP outperformed all other models when producing the lowest mean squared error (MSE).

Zhang et al. developed a model that simultaneously predicts car-following and lane-changing behaviors using deep learning (X. Zhang et al., 2019). They used the historical positions (lateral and longitudinal coordinates) of six vehicles surrounding the subject vehicle to predict the position of the subject vehicle. They used the I-80 database gathered from NGSIM and developed an LSTM-based model which was further optimized by the hybrid retraining constrained (HRC) method. The model was validated by the US-101 highway dataset. The proposed HRC LSTM produced less prediction error than the traditional LSTM model (error drops from 0.094 to 0.049).

Tang et al. combined the Markov chain theory and the GRU algorithm to develop a car-following model named the MG model (Tang et al., 2020). The model predicts velocity and space headway by analyzing the historical data of 10-time steps. They used the US-101 highway (*NGSIM*, 2016) keeping vehicles with a length of less than 5 m in the first and second lanes. The proposed one-step prediction model (MG model) outperformed FNN and regular GRU models in accuracy, improving the stability of the car-following phenomena.

Hart et al. proposed a reward-based deep learning algorithm called Reinforcement Learning (RL) to develop a car-following model that considers both free driving and car-following situations (Hart et al., 2021). Two distinct RL policies had been implemented for free driving and car-following states. The free-driving policy aims to reach and not exceed a certain desired speed and the car-following policy aims to maintain the desired safety gap between successive vehicles. A separate reward function was developed for each RL policy where different driver characteristics can be modeled by adjusting the parameters of the reward functions. The proposed model was then compared with IDM and found to be more stable, safe, and reliable than IDM.

2.5 Summary of the Literature Review

In summary, the literature review provided the impact of semi-automated vehicles on driving behavior, and presented various car-following models. Various studies nowadays are implementing new strategies to improve SAVs and make these systems more comfortable and safer. However, especially for level 2 or 3 automation, CTs may create unsafe situations. A CT is a state when a driver switches from an automated mode to a manual mode and vice-versa. Applying any amount of force on the brake pedal will disengage ACC while driving an SAV. In various critical situations, drivers are forced to apply the brake because of the increased risk and disengage the ACC. This kind of situation can also decrease the trust of the drivers in the ACC. Therefore, to improve the ACC system and make the drivers feel safe and risk-free, it is crucial to investigate how differently the ACC system can have an impact on heterogenous mass of people so that it can be efficiently and equitably improved in future. Researchers have developed algorithms to predict the longitudinal behavior of both manually-driven vehicles and SAVs. The literature provides several comparisons of the car-following models for manual vehicles where

IDM showed the best performance among the other models. Recent developments in AI enable researchers to study car-following behaviors more accurately. Depending on the gathered data and the scope of the study, different studies implemented various deep learning algorithms (CNN, DNN, LSTM, RNN, etc.) to predict the car-following behavior of the driver. These deep-learning models showed better performance than IDM in terms of stability, safety, and reliability.

Chapter 3 Methodology

The current ACC system that is equipped in SAVs has performance shortcomings related to the safety and comfort of the driver. In sudden critical traffic conditions, such as aggressive merging from an on-ramp, or sudden cut-in between the subject and preceding vehicles, the ACC often fails to produce the appropriate deceleration that is needed to avoid a collision, thus the CT (automated to manual) takes place.

In this study novel ensemble ML models have been used to predict the CT of ACC-equipped vehicles. From these models, the situation when the ACC transition occurs can be explored.

3.1 Prediction Models

To date, there are numerous ML prediction models available. However, there are benefits and drawbacks in using any ML model, depending on the problem and the type of data used to train them. Ensemble learning is a type of ML approach that integrates several individual models to create a more robust and precise prediction model. Individual models have different shortcomings while handling complex data and patterns and may specialize in different aspects of the data. The ensemble learning technique combines all models to enable a more comprehensive depiction of the underlying patterns and overcomes the drawbacks of individual models, like reducing overfitting and handling complexity (Rokach, 2019; Sagi & Rokach, 2018; Sewell, 2008). There are two types of algorithms for ensembled learning ML models: (a) Bootstrap Aggregating (Bagging), and (b) Boosting.

3.1.1 Bootstrap Aggregating (Bagging)

The Bagging algorithms perform random sampling with replacement on the entire training data set to generate numerous subsets. The base models are trained independently on each subgroup, and then their outputs are combined to produce the final prediction.

The Random Forest (RF) algorithm (Breiman, 2001; *Random Forests | SpringerLink*, n.d.) is a highly adaptable ML technique that falls under this category. This bagging ensemble technique uses decision trees as its base model and predicts by combining the predictions of several decision trees. The construction of each decision tree involves the random selection of subsets of the training data via bootstrapping. The RF algorithm is recognized for its ability to avoid overfitting, due to the ensemble averaging technique that reduces the influence of errors in individual trees (Biau & Scornet, 2016; Breiman, 2001; Cutler et al., 2012).

Bagging algorithms reduce variance and mitigate overfitting by training multiple models in parallel on a variety of data subsets, hence enhancing the robustness of the models. Moreover, the utilization of bagging techniques mitigates the impact of outliers and noisy data on the model. Additionally, bagging is a computationally efficient technique that is particularly well-suited for handling huge datasets and complex models. Nevertheless, bagging does have several disadvantages, including higher model complexity and limited improvements for models that are already stable. The efficacy of bagging is contingent upon the specific attributes of the dataset and the underlying base learning method employed.

3.1.2 Boosting

Boosting is a widely used ensemble learning method that aggregates several weak learners to construct a robust predictive model. The boosting method aims to enhance the

efficacy of several base models by progressively assigning greater significance to incorrectly classified events.

The training cycle begins with distributing equal weights to each instance. After training the base learner, misclassified cases are weighted higher to emphasize the hard-to-predict occurrences. Each iteration trains more base learners and emphasizes the misclassified occurrences from the previous iteration (Al Daoud, 2019; Sewell, 2008). The Extreme Gradient Boosting (XGBoost) and Light Gradient Boosting Machine (LightGBM) algorithms are the most popular and vastly used in various fields.

By sequentially concentrating on misclassified instances, boosting improves the accuracy of the model. Moreover, by emphasizing misclassifications and enhancing generalization, boosting mitigates overfitting. Although boosting can handle and improve weak learners, it creates complex models which takes a long time to train and sometimes can be challenging to interpret.

3.1.2.1 XGBoost

XGBoost is a cutting-edge ML algorithm with exceptional predictive ability, scalability, and adaptability. It was developed by Chen and Guestrin in 2016 (Chen & Guestrin, 2016) and since then it is widely used due to its high-scale dataset handling capacity, quick implementation, and regularization approaches. XGBoost's core concept is to iteratively add weak models to the ensemble by optimizing a particular objective function. At each iteration, the algorithm computes the negative gradient of the loss function relative to the present ensemble predictions. These values are used to build a new weak model that minimizes the objective function shown in equation 3.1:

$$Obj = \sum_{i=1}^{n} L(y_i, \hat{y}_i) + \sum_{k=1}^{K} \Omega(f_k) \tag{3.1}$$

Where, $L(y_i, \hat{y}_i)$ is the training loss, which measures the performance of the model in training data; $\Omega(f_k)$ is the regularization term, which controls the model complexity for preventing overfitting; n is the volume of training datasets, and K is the number of trees.

3.1.2.2 LightGBM

This technique first provides the model with a starting point estimate. Then, a robust ensemble of decision trees is built one at a time by successively minimizing a given loss function. The flaws in former trees are fixed in the construction of succeeding ones. Unlike traditional gradient-boosting algorithms that grow trees in a depth-first manner, LightGBM grows trees leaf-wise (Yan et al., 2021). This means that the leaves with the biggest loss reduction are the ones that are divided, which leads to more efficient and faster training, and better accuracy.

The objective function, which specifies the loss to be minimized during training, is a crucial part of LightGBM. It combines a regularization term that helps prevent overfitting with a differentiable loss function (Shi et al., 2019). To minimize the remaining errors, it determines the negative gradients of the loss function relative to the existing model's prediction and then fits a new tree (Wen et al., 2021). The new tree's predictions are subsequently included into the old ensemble, which improves over time. The update phase of LightGBM is mathematically described as:

$$\hat{y}_i^{(t)} = \hat{y}_i^{(t-1)} + \gamma \sum_{j=1}^{J} w_j . h_j(x_i) \tag{3.2}$$

Where, $\hat{y}_i^{(t)}$ and $\hat{y}_i^{(t-1)}$ represent the updated and previous prediction respectively for the *i*-th instance at *t* iteration; w_j represents the weight assigned to leaf *j*; and $h_j(x_i)$ is the prediction of the *j*-th tree on the instance x_i.

3.2 Inputs and Output

From the driving data of 30 participants, variables related to the vehicle trajectories, such as velocity, headway (space and time), acceleration, lane deviation, etc. have been extracted. Additionally, demographic information such as gender, age, and experience, have been collected from the survey questionnaire. The driving simulator data also provided the indicators of when the CTs occurred during the driving of 30 participants. A total of 320 CTs were extracted from all the participants' data where they used the brake to disengage ACC and took over the control of the vehicle. The output of the CT model was the indicator of CT which is a dummy variable. The time a participant pressed the brake to disengage the ACC, the dummy variable became '1', otherwise the value was '0' (when the ACC was turned on). The inputs for the CT prediction can be divided into three categories: vehicle trajectories, driver demographics, and psychological parameters.

3.2.1 Vehicle trajectories: simulator data

Time series information of vehicle velocity (v), front vehicle's (preceding vehicle) velocity (v_l), time headway (t_h), and lane deviations (ld) were extracted from the simulator. The relative velocity (v_r) was estimated by calculating the differences between the driver's vehicle's and preceding vehicles' velocities ($v - v_l$).

3.2.2 Driver demographics: survey questionnaires

A pre-driving questionnaire was required to be filled out before the driving experiment. Demographic information of the participants such as age, gender, years of having a driving license, and years of experience driving with ACC were collected from the survey data.

3.2.3 Psychological parameters: eye-tracker data

The eye-tracker device monitored the eye movement of the drivers in real time throughout the drive. Using the pupil diameter, eyelid opening, and pupil movements the device calculated the subjective workload. Subjective workload refers to an individual's perception of the mental and physical effort needed to complete an activity. It relies on subjective assessment and might differ among persons, even when performing an identical activity.

3.3 Performance Metrics

To evaluate the performance of the tested ML algorithms, different performance metrics from the confusion matrix were explored, which were calculated based on true positive (TP), true negative (TN), false positive (FP), and false negative (FN) outcomes.

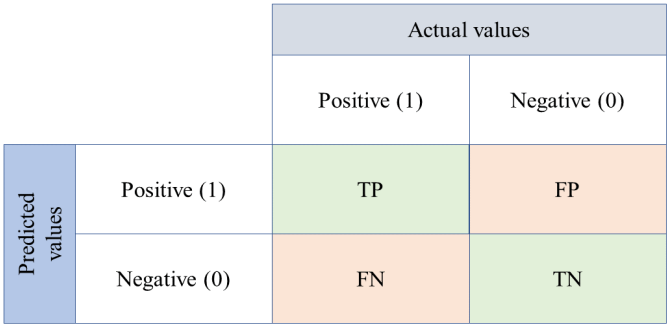

Figure 3.1 Confusion matrix

From the confusion matrix (Figure 3.1) the overall accuracy (ACC), Precision (P), Recall (R), and F1-score (F) were calculated based on equations 3.3 through 3.6.

Accuracy (ACC): Overall accuracy of the model.

$$ACC = \frac{TP + TN}{TP + TN + FP + FN} \tag{3.3}$$

Precision (P): The proportion of positive identification that was actually correct.

$$\mathrm{P} = \frac{\mathrm{TP}}{\mathrm{TP} + \mathrm{FP}} \tag{3.4}$$

Recall (R): The fraction of relevant instances that were retrieved, also known as "sensitivity".

$$\mathrm{R} = \frac{\mathrm{TP}}{\mathrm{TP} + \mathrm{FN}} \tag{3.5}$$

F-score (F): Precision and recall ratings are typically combined and not mentioned separately. The F1-score, which is the harmonic mean of the accuracy and recall, is the most practical value to use when describing a model's performance.

$$F1 = \frac{2\mathrm{PR}}{\mathrm{P} + \mathrm{R}} \tag{3.6}$$

Another performance metric that has been utilized in this research is the Receiver Operating Characteristic (ROC) Area Under the Curve (AUC) value. The ROC-AUC value signifies the extent of the area beneath the ROC curve, which spans from 0 to 1. A greater ROC-AUC value, approaching 1, indicates that the model possesses a higher likelihood of assigning a higher rank to a randomly selected positive sample compared to a randomly selected negative sample.

Chapter 4 Data Collection

This research used the KU driving simulator, a miniSim PC-based National Advanced Driving Simulator (NADS) (*Simplified Cab miniSim - miniSim*, n.d.). The KU driving simulator provides a 170-degree horizontal view with three forward screens (front view, left view, and right view) and one rear screen (for side mirror views and rear mirror view) (fig. 4.1).

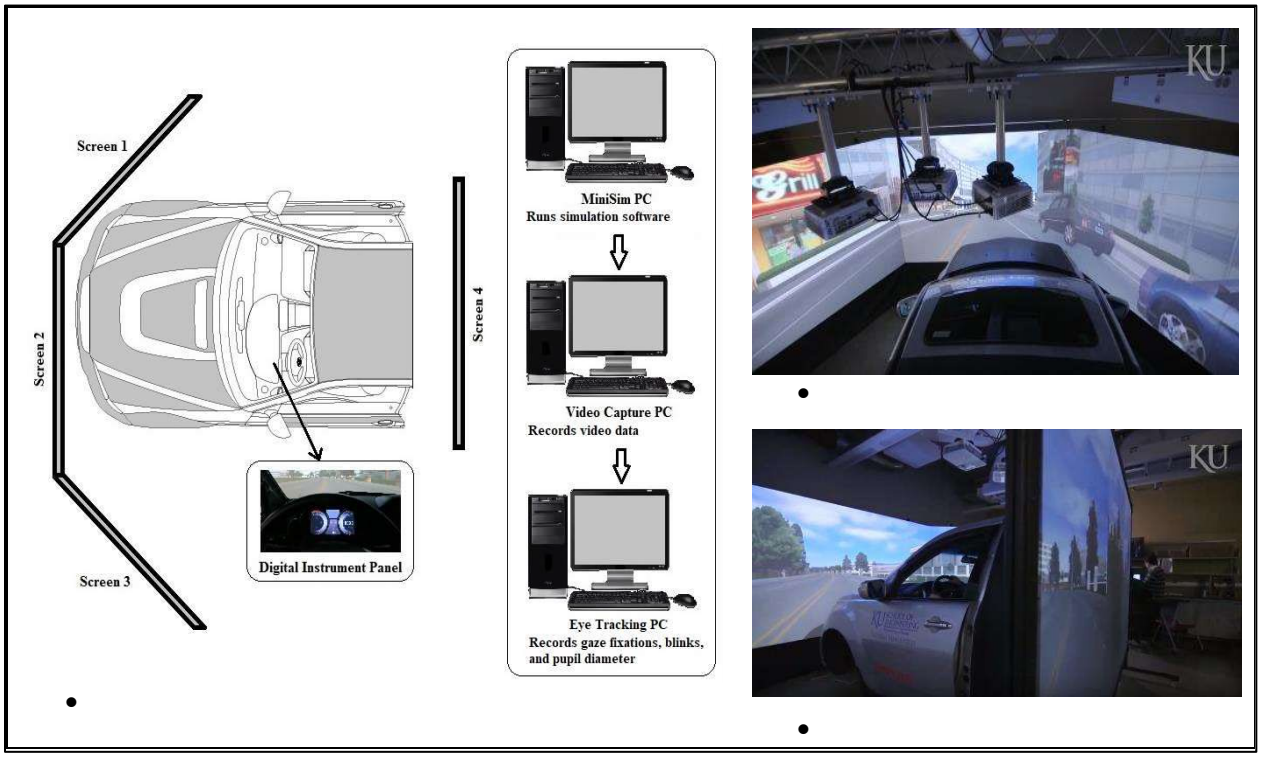

Figure 4.1 KU driving simulator layout (Kummetha et al., 2020)

The simulator cab has four high-definition (HD) cameras inside of it. The VidCap PC captures the movements of the participant, braking behavior, steering wheel activity, and facial expressions from the inside cameras. Additionally, an eye tracker is equipped inside the vehicle to measure eye movements and subjective workload through pupil diameter and eyelid opening. The KU simulator is equipped with SAE level 2 automation feature, ACC. In this study, each

participant drove in both manual and SAV conditions. The data frequency extracted from the simulator was 60 Hz and from the eye-tracker, the workload data frequency was 10 Hz. The eye-tracker data were converted from 10 Hz to 60 Hz to match the two datasets. After matching the frequencies, the data extracted from the simulator and eye-tracker were combined for each participant.

4.1 Scenario Development

To build various scenarios, first, the roadway design was developed by using the Tile Mosaic Tool (TMT) where several road tiles are connected to build required road segments. After building road segments, the Interactive Scenario Authoring Tool (ISAT) was used to build the driving scenarios and environments. Both TMT and ISAT simulator software have been developed by NADS. The miniSim will run the assembled scenario and collect the data.

To capture the driver's reaction in risky situations, one free-flow driving and eight car-following scenarios on a two-lane road segment were developed for both manual and SAV driving conditions. The speed limit has been set to 70 mph. The scenarios were combinations of different traffic densities, percentages of heavy vehicles, roadway construction, vehicle cut-in, and aggressive merging from the on-ramp. This study focused on three types of car-following situations that can cause CTs: vehicle cut-in, merging from the on-ramp, and lane drop for construction.

4.1.1 Scenario 1: Base Drive

Scenario 1 was developed to obtain the base driving of the participants while driving without ACC (speeding, acceleration, etc.) and also the preferred time gap and set-up velocity while driving with ACC. There were no other vehicles on the road (fig 4.2).

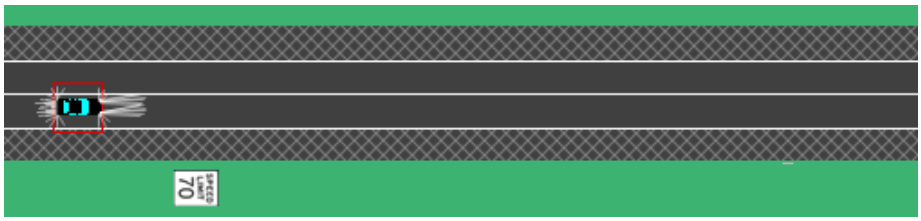

Figure 4.2 Base drive scenario

4.1.2 Scenario 2: Vehicle Cut-In

In this car-following situation, a vehicle from the adjacent lane tries to cut in between the following and preceding vehicles (fig 4.3). This sudden cut-in was simulated through various combinations of traffic density and percentages of heavy vehicles.

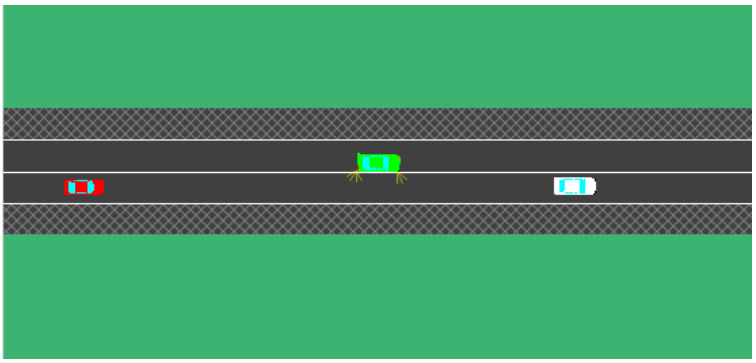

Figure 4.3 Vehicle cut-in scenario

4.1.3 Scenario 3: Merging from the On-ramp

While driving in a car-following condition, a vehicle from the on-ramp segment merges into the main lane between the subject and the preceding vehicle (in front of the driver). Similar to the cut-in scenario, this situation was also simulated through various combinations of traffic density and heavy vehicle percentages (fig 4.4).

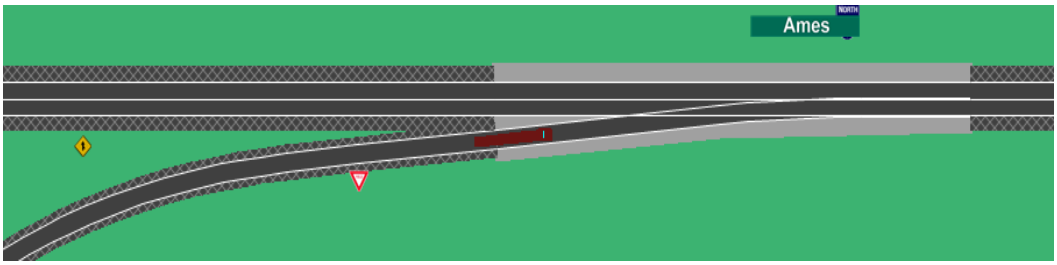

Figure 4.4 Merging layout scenario

4.1.4 Scenario 4: Lane Drop

In this scenario, while driving in car-following conditions, the driving lane was closed due to roadway construction. In this situation, the driver will have to press the brake and change the position of the vehicle to the adjacent lane (fig 4.5). This situation was also simulated through various combinations of traffic density and heavy vehicle percentages.

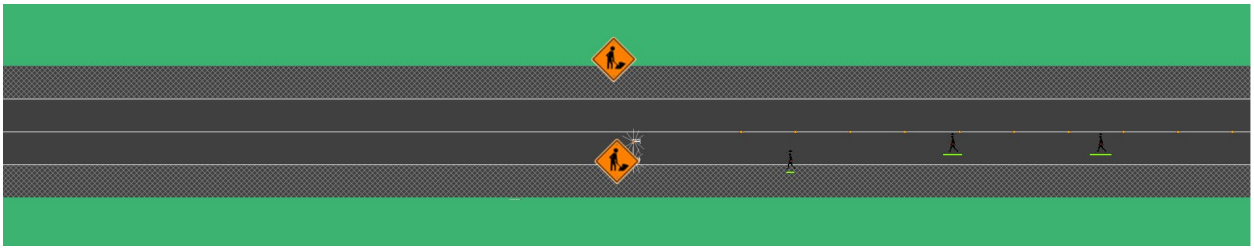

Figure 4.5 Lane drop due to construction scenario

The entire duration of the simulation was 17 minutes for each level of vehicle automation (34 minutes total). The summarized scenarios are listed in Table 4.1.

Table 4.1 Summary of driving scenarios for manual driving and semi-automated driving

Task	Density	Percentage of Heavy vehicles	Lane change per km/lane	Lane drop	Merging from on-ramp	Time (min)
General (baseline)	0	0	0	0	0	1
Car-Following	Low	0	1	0	0	1
Car-Following	Low	0	0	0	1	2
Car-Following	Low	0	0	1	0	1
Car-Following	Medium	10	2	0	0	2
Car-Following	Medium	10	0	0	1	2
Car-Following	High	10	2	0	0	3
Car-Following	High	20	0	1	0	2
Car-Following	High	20	0	0	1	3

While running these scenarios to capture the reactions of the participants, several variables related to vehicle trajectories, driver characteristics and physiology including driver's reactions were collected to build the CT model. Table 4.2 shows the summarized variables that were collected for this research.

Table 4.2 Summarized data collection

Variables to be collected	Data collection method
Velocity of the subject vehicle *(v)*	Output from the MiniSim
Velocity of the preceding vehicle *(v_l)*	Output from the MiniSim
Acceleration of the subject vehicle *(a)*	Output from the MiniSim
Time headway *(t_h)*	Output from the MiniSim
Space headway *(h)*	Output from the MiniSim
Mental workload *(WL)*	From Eyetracker
Driver's characteristics: Age, Gender, Experience, Years of driving license, Automation experience *(DrCh)*	Pre-driving (screening) questionnaires

4.2 Participants Recruitment

The study was first submitted to the Human Research Protection Program (HRPP) at the University of Kansas (KU) for approval. After getting approval, the study was advertised through flyers, social media, and e-mail announcements for recruiting participants. A total of 30 participants were recruited to participate in this research, equally split between males and females. Participants were screened using a pre-driving questionnaire and selected if they were between the ages of 18 and 65 years, with at least three years of driving experience, valid U.S. driver's license, annual mileage no less than 5,000 miles, and in good health (free from seizures, eye conditions, ear problems, heart conditions, arthritis, excessive motion sickness, and the possibility of pregnancy). A $40 gift was provided to the participants after the completion of the study as compensation for their time.

Chapter 5 Results and Analysis

5.1 Exploratory Data Analysis

We investigated the differences in driving performances between non-automated and semi-automated driving conditions. Figure 5.1 shows that the average time headway was higher in ACC for each age group. The older age group (group 3) tends to keep higher headway than the other groups. The average time headway of age group 2 was lower than group 1 in manual driving, but higher in the ACC driving condition.

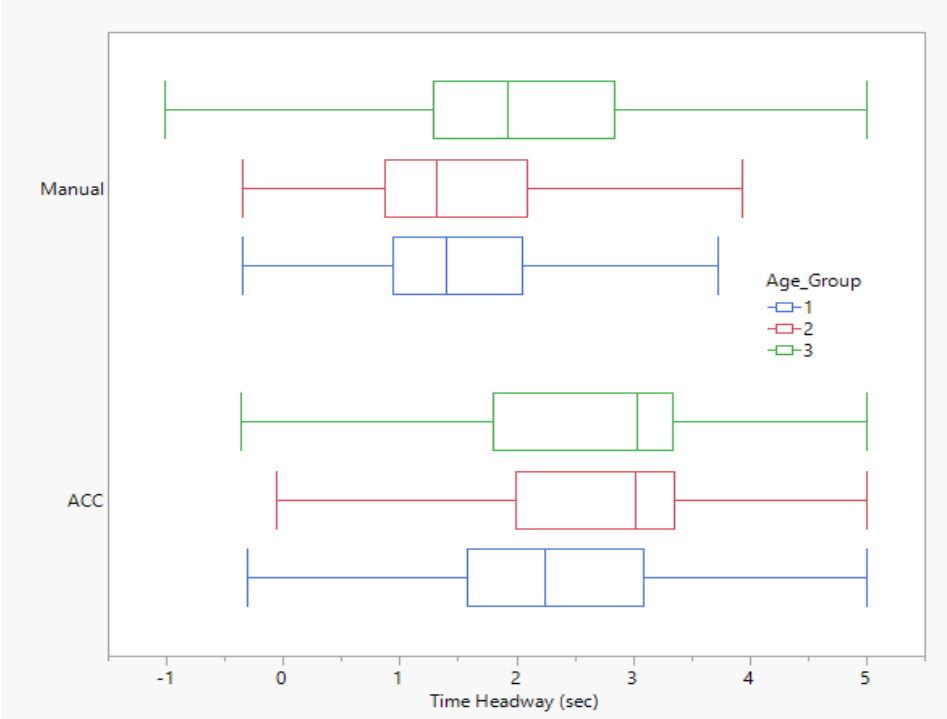

Figure 5.1 Boxplot of time headway across different age group

Figure 5.1 shows that male participants maintained higher headway than females in manual driving, but in ACC drive, a significant shift in average time headway can be seen in female participants' driving which was greater than males.

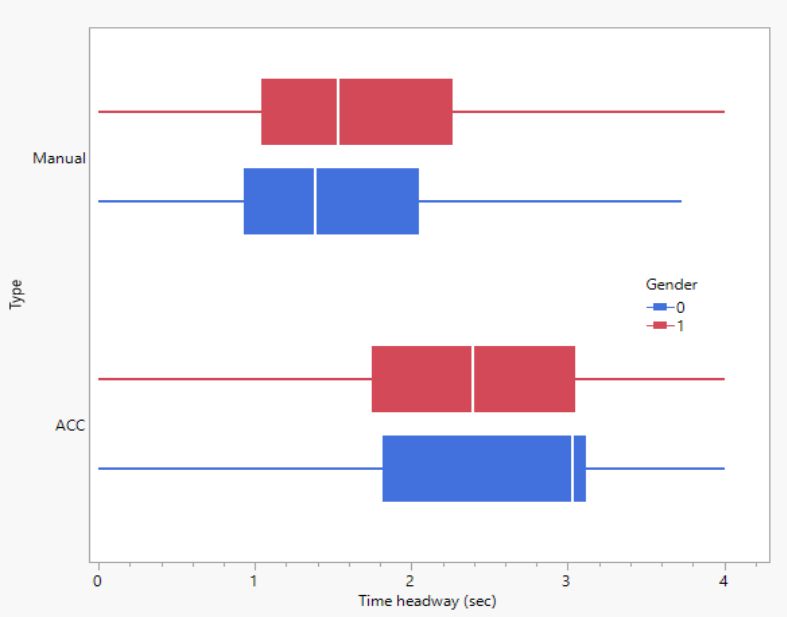

Figure 5.2 Boxplot of time headway across different genders (1=Male, 0=Female)

The average and standard deviation (SD) of the speed was lower in manually driven conditions (mean=93.96 ft/s, SD=11.97) than in ACC-driven conditions (mean=94.60 ft/s, SD=14.35). When the lead vehicle velocity was lower than 60 ft/s the average acceleration was lower in ACC than manual drive but at a higher speed, the acceleration was higher in manual drive than ACC (Figure 5.3).

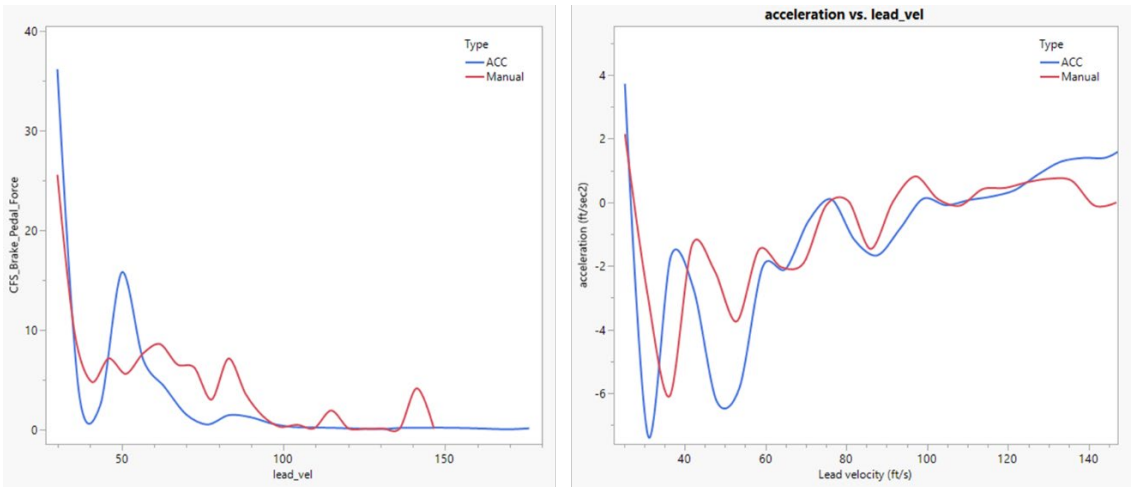

Figure 5.3 Relationship of acceleration and brake pedal force with the lead vehicle's velocity.

Figure 5.3 also shows that, whenever the lead vehicle's velocity was lower, the participants on average applied higher force on the brake pedal in the ACC condition than in the manual condition. Even though ACC was created to produce appropriate deceleration by itself to make the driver feel safer, the participants' average and maximum brake pedal force was higher in ACC than in manual conditions (Figure 5.4) which reflects the poor braking performance of the ACC system that led CT to occur.

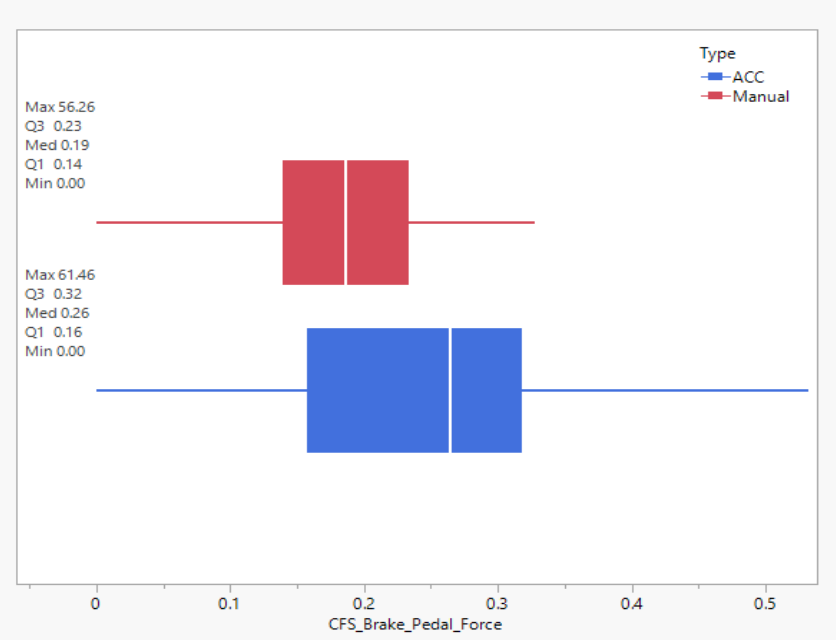

Figure 5.4 Boxplot of brake pedal forces in ACC and manual driving condition

The workload was calculated from the eye-tracker device which used the pupil diameter and eye movements to quantify subjective workload. Figure 5.5 shows that the subjective workload was lower in the ACC driving condition than the non-automated driving although the maximum value of workload was higher in the ACC driving condition. It indicates that participants were relatively less aware and perceived less risk in ACC driving, but when a sudden risky situation was raised, the workload increased sharply which also led the brake pedal forces to be greater than the manual driving condition.

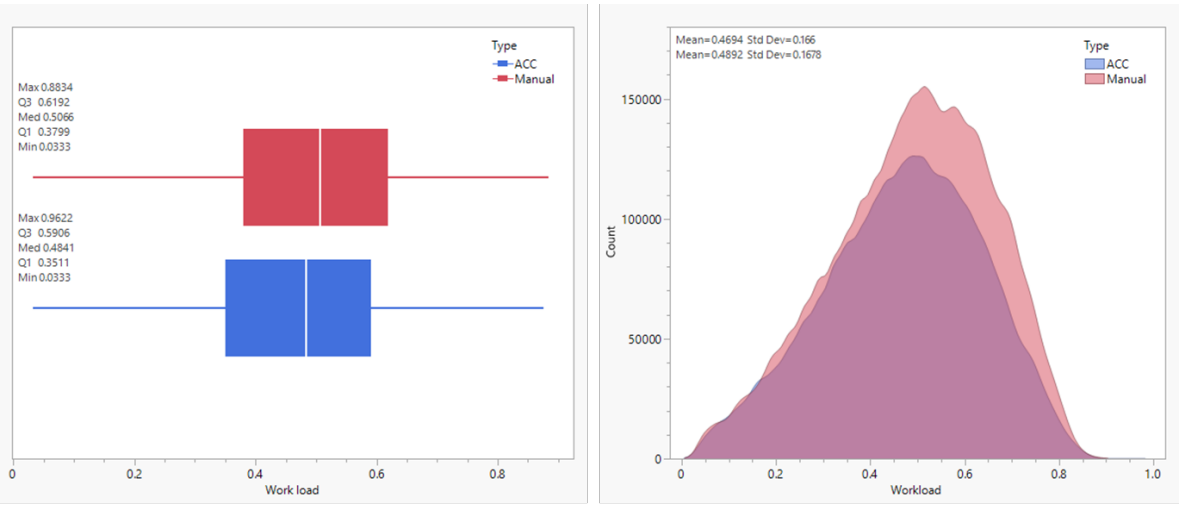

(a) (b)

Figure 5.5 Boxplot (a) and kernel density (b) of workload in ACC and manual driving conditions

The ACC CT behavior was found to be different across different age groups and genders. Figure 5.6 shows that although the CT occurred mostly in male participants' driving at age groups 1 and 2, this rate was proportional for males and females in age group 3.

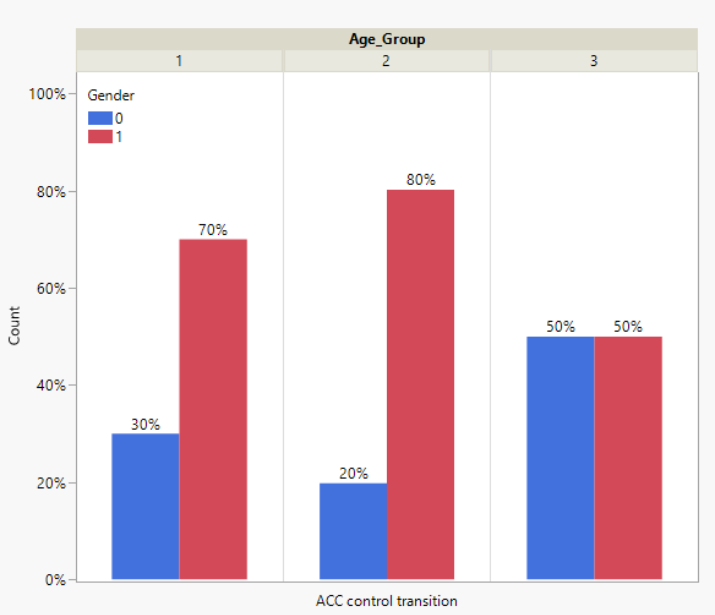

Figure 5.6 CT across different demographics

Figure 5.7 depicts the relationship of CT with the relative velocity (own velocity – preceding velocity) and space headway for males and females. From this figure it can be seen that at higher relative velocity and lower space headway, the male participants tend to perform CT more than female participants.

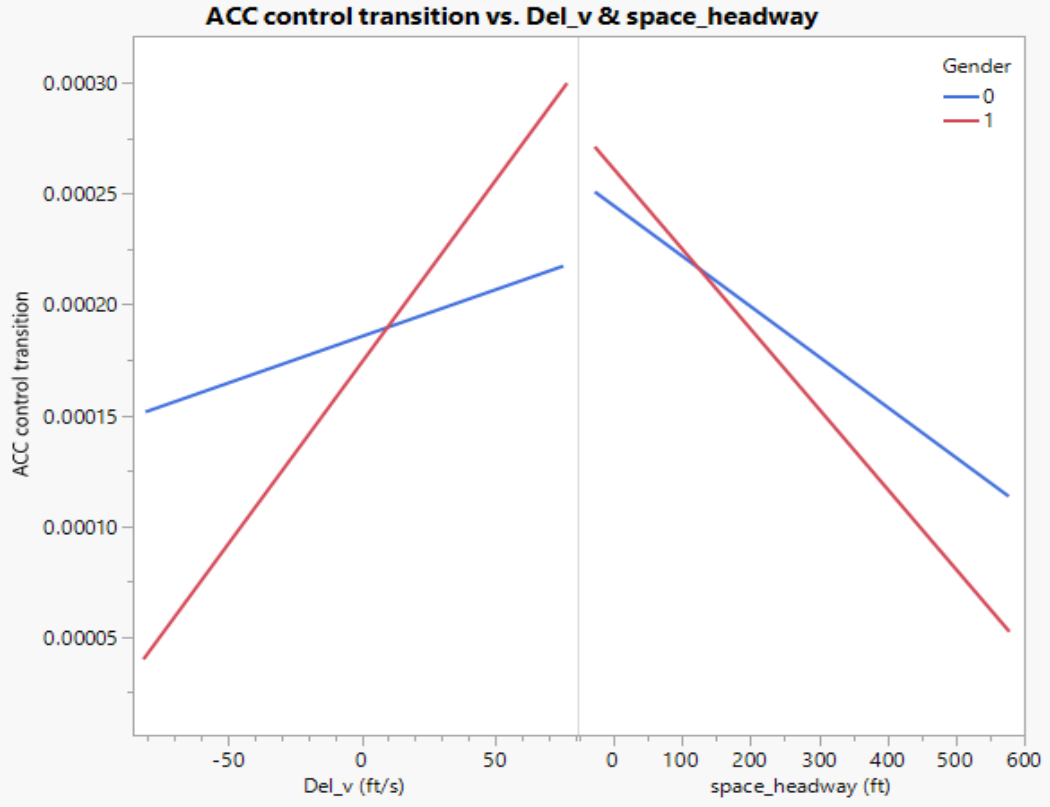

Figure 5.7 Impact of relative velocity and space headway on ACC CT

5.2 Model Performances

The models' comparison is summarized in Table 5.1. Their performance was evaluated on unseen test datasets to get the models' reliability in real-world scenarios. The higher ROC-AUC value indicates enhanced performance in terms of the differentiation between classes and the model accuracy. A higher F1 score suggests that the model demonstrated a stronger performance in accurately identifying positive instances and effectively avoiding misclassifications compared to other prediction models. From Table 5.1 it can be seen that boosting-based ensemble ML models performed better than the bagging ensemble ML model (RF). Among the three models, XGBoost produced the best performances with accuracy, F-1 score, and ROC_AUC values of 0.75, 0.83, and 0.76 respectively.

Table 5.1 Model performances

Model Type	Model Name	Accuracy	ROC-AUC	F1 score
Boosting-based ensemble ML	LightGBM	0.74	0.82	0.74
Boosting-based ensemble ML	XGBoost	**0.75**	**0.83**	**0.76**
Bagging ensemble ML	Random Forest (RF) Classifier	0.71	0.74	0.71

5.3 Factors Associated with CT

The interpretability of ML models has been a limitation in understanding their predictions. To address this limitation, Lundberg and Lee introduced a new approach called "SHapley Additive exPlanations" (SHAP) analysis, which aims to explain the impact of input variables on the model's output (Lundberg & Lee, 2017). In this study, the SHAP analysis was performed for the XGBoost since it produced the highest prediction performance.

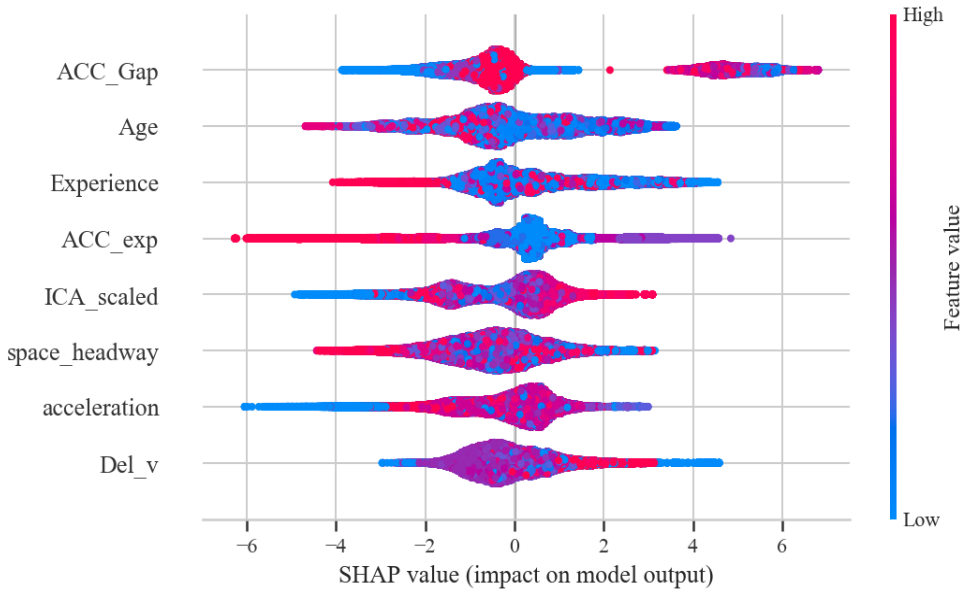

Figure 5.8 SHAP analysis of ACC CT model

The blue and red colors in Figure 5.8 represents the lower and higher values, respectively, of a feature and the x-axis shows the SHAP value of the feature. From this figure, we found that participants using the lowest ACC gap setting had relatively lower CTs than other settings. Age did not show a settled relationship with CT, but younger participants tended to perform CT a bit more than older adults. Both experience in driving and the ACC system had a huge impact. CTs were mostly found in the driving of less experienced drivers. A positive relationship was extracted between the subjective workload (ICA_scaled) and CT. It indicates that the higher the subjective workload, the higher the chance of a CT occurrence. Among the vehicle trajectory parameters from the figure, although headway shows an inverse relationship with CT, this relationship is not firm. This is because the CT can happen in sudden change of scenarios, which might not reflect in all the trajectory parameters. Similarly, acceleration was not found to have a clear relationship with CT. However, higher relative velocity was found as one of the key factors behind CT. This indicates that, whether a driver is driving in a higher speed and acceleration or lower, the CT mostly depends on the front vehicle's velocity, perceived workload, and experience with the system and driving. These visual representations describe, on a global scale, how each characteristic contributes to the average model forecast of the ACC CT.

Chapter 6 Conclusion and Future Recommendations

This research investigated the CT from automatic to manual driving in SAVs, with an emphasis on ACC technology. Given the growing adoption of SAVs, it is imperative to comprehend the circumstances and timing in which drivers adapt their behavior when they take control of automated systems. Such understanding is vital for improving safety and boosting the overall driving experience. The study investigated the driving behavior of 30 participants in a driving simulator across several driving conditions, such as sudden vehicle cut-ins, merging from on-ramps, and lane reductions caused by construction. Various combinations of the vehicle density and percentage of heavy vehicles were deployed in those driving scenarios. The study utilized ensemble ML algorithms, such as RF, XGBoost, and LightGBM, to predict and analyze the CTs that occurred driving with ACC using vehicle trajectory data, driver demographics, and psychological parameters. The findings revealed that the ACC cannot always provide the required deceleration when unexpected critical situations occur, resulting in CTs.

Among the three ensemble ML models used in this study, the gradient boosting algorithm XGBoost showed the best performance with the accuracy, F1 score, and ROC_AUC score of 0.75, 0.83, and 0.76 respectively. After selecting the best model, the SHAP analysis was conducted on that model. SHAP analysis was performed to explore the relationship between the prediction with the predictors and identify key factors influencing CTs. The analysis suggests that CT is not entirely related to the vehicle velocity and acceleration but rather mostly related to the preceding vehicle's trajectories, and the driver's perceived workload. Moreover, CT mostly occurred in lower space headway although that relationship is not always true. CT can occur in various space headways and accelerations, depending on the state of drivers' mental capacity, workload, demographics, and relative velocity. When the relative velocity is higher, that

indicates a sudden decrease in the front vehicle's velocity and it is irrespective of the speed of the vehicle was driving. It is crucial to understand the impact of the subjective workload on CT. The study revealed that driving with ACC lowers the perceived workload which indicates drivers were relaxed, less aware, and perceived less risk. The CT mostly occurred in sudden critical conditions for which the drivers were not ready. The mental workload increased to a great extent in a very short time during those sudden critical conditions that led the CT to occur. Additionally, some of the driver demographics showed some important relationships with CT. Although gender did not have any impact on CT, the experience with the ACC system and overall driving were found to be significant factors for CT. Less experienced drivers were more likely to perform CT. Similarly, less experience with the ACC system led to more CT, indicating that, in particular critical situations, less experienced drivers show less trust in the ACC system.

Due to the substantial impact of mental workload on CTs, it is recommended to improve the ACC systems in SAVs by integrating more sensors and algorithms related to human factors. This enhancement would enable the systems to anticipate and react more effectively to unexpected risky occurrences, such as aggressive merging or cut-ins. As a result, the frequency of CTs would decrease, leading to enhanced safety. Moreover, specialized driver training programs can be implemented to enhance drivers' comprehension and understanding to manage the limitations of ACC systems, enabling them to respond effectively in unforeseen circumstances. Future research should explore the integration of additional variables, such as weather conditions and road surface quality, into predictive models, and test these models in real-world driving scenarios for more comprehensive insights. When developing and overseeing ACC systems in SAVs, policymakers, and vehicle manufacturers can consider the findings from

this research. It is important to test these systems in different real-world scenarios to promote the development of safer and more dependable automation technology.

References

Al Daoud, E. (2019). Comparison between XGBoost, LightGBM and CatBoost using a home credit dataset. *International Journal of Computer and Information Engineering*, *13*(1), 6–10.

Biau, G., & Scornet, E. (2016). A random forest guided tour. *Test*, *25*, 197–227.

Biondi, F. N., Lohani, M., Hopman, R., Mills, S., Cooper, J. M., & Strayer, D. L. (2018). 80 MPH and out-of-the-loop: Effects of real-world semi-automated driving on driver workload and arousal. *Proceedings of the Human Factors and Ergonomics Society Annual Meeting*, *62*(1), 1878–1882.

Boer, E. R. (2001). Behavioral entropy as a measure of driving performance. *Proceedings of the First International Driving Symposium on Human Factors in Driver Assessment, Training and Vehicle Design*, 225–229.

Breiman, L. (2001). Random forests. *Machine Learning*, *45*, 5–32.

Calvi, A., D'Amico, F., Ferrante, C., & Ciampoli, L. B. (2020). A driving simulator study to assess driver performance during a car-following maneuver after switching from automated control to manual control. *Transportation Research Part F: Traffic Psychology and Behaviour*, *70*, 58–67.

Chandler, R. E., Herman, R., & Montroll, E. W. (1958). Traffic Dynamics: Studies in Car Following. *Operations Research*, *6*(2), 165–184. https://doi.org/10.1287/opre.6.2.165

Chen, T., & Guestrin, C. (2016). XGBoost: A Scalable Tree Boosting System. *Proceedings of the 22nd ACM SIGKDD International Conference on Knowledge Discovery and Data Mining*, 785–794. https://doi.org/10.1145/2939672.2939785

Cutler, A., Cutler, D. R., & Stevens, J. R. (2012). Random forests. *Ensemble Machine Learning: Methods and Applications*, 157–175.

Davis, L. C. (2004). Effect of adaptive cruise control systems on traffic flow. *Physical Review E*, *69*(6), 066110.

De Winter, J. C., Happee, R., Martens, M. H., & Stanton, N. A. (2014). Effects of adaptive cruise control and highly automated driving on workload and situation awareness: A review of the empirical evidence. *Transportation Research Part F: Traffic Psychology and Behaviour*, *27*, 196–217.

Fellendorf, M., & Vortisch, P. (2010). Microscopic traffic flow simulator VISSIM. In *Fundamentals of traffic simulation* (pp. 63–93). Springer.

Fuller, R. (2005). Towards a general theory of driver behaviour. *Accident Analysis & Prevention*, *37*(3), 461–472. https://doi.org/10.1016/j.aap.2004.11.003

Gazis, D. C., Herman, R., & Rothery, R. W. (1961). Nonlinear follow-the-leader models of traffic flow. *Operations Research*, *9*(4), 545–567.

Gipps, P. G. (1981). A behavioural car-following model for computer simulation. *Transportation Research Part B: Methodological*, *15*(2), 105–111. https://doi.org/10.1016/0191-2615(81)90037-0

Han, D., & Yi, K. (2006). A driver-adaptive range policy for adaptive cruise control. *Proceedings of the Institution of Mechanical Engineers, Part D: Journal of Automobile Engineering*, *220*(3), 321–334.

Hart, F., Okhrin, O., & Treiber, M. (2021). Formulation and validation of a car-following model based on deep reinforcement learning. *arXiv Preprint arXiv:2109.14268*.

Herman, R., Montroll, E. W., Potts, R. B., & Rothery, R. W. (1959). Traffic dynamics: Analysis of stability in car following. *Operations Research*, *7*(1), 86–106.

Huang, X., Sun, J., & Sun, J. (2018). A car-following model considering asymmetric driving behavior based on long short-term memory neural networks. *Transportation Research Part C: Emerging Technologies*, *95*, 346–362. https://doi.org/10.1016/j.trc.2018.07.022

Inagaki, T., & Sheridan, T. B. (2019). A critique of the SAE conditional driving automation definition, and analyses of options for improvement. *Cognition, Technology & Work*, *21*(4), 569–578. https://doi.org/10.1007/s10111-018-0471-5

International, S. (2018). Taxonomy and definitions for terms related to driving automation systems for on-road motor vehicles. *SAE*.

Jurgen, R. K. (2006). *Adaptive cruise control*. SAE Technical Paper.

Kesting, A., Treiber, M., Schönhof, M., & Helbing, D. (2007). Extending adaptive cruise control to adaptive driving strategies. *Transportation Research Record*, *2000*(1), 16–24.

Kometani, E., & Sasaki, T. (1959). A safety index for traffic with linear spacing. *Operations Research*, *7*(6), 704–720.

Kummetha, V. C., Kondyli, A., & Schrock, S. D. (2020). Analysis of the effects of adaptive cruise control on driver behavior and awareness using a driving simulator. *Journal of Transportation Safety & Security*, *12*(5), 587–610. https://doi.org/10.1080/19439962.2018.1518359

Leutzbach, W. (1988). *Introduction to the theory of traffic flow* (Vol. 47). Springer.

Lundberg, S. M., & Lee, S.-I. (2017). A unified approach to interpreting model predictions. *Advances in Neural Information Processing Systems*, *30*.

Luo, L., Liu, H., Li, P., & Wang, H. (2010). Model predictive control for adaptive cruise control with multi-objectives: Comfort, fuel-economy, safety and car-following. *Journal of Zhejiang University SCIENCE A*, *11*(3), 191–201.

Ma, R., & Kaber, D. B. (2005). Situation awareness and workload in driving while using adaptive cruise control and a cell phone. *International Journal of Industrial Ergonomics*, *35*(10), 939–953. https://doi.org/10.1016/j.ergon.2005.04.002

Manawadu, U. E., Kawano, T., Murata, S., Kamezaki, M., Muramatsu, J., & Sugano, S. (2018). Multiclass classification of driver perceived workload using long short-term memory based recurrent neural network. *2018 IEEE Intelligent Vehicles Symposium (IV)*, 1–6.

Miller, E. E., & Boyle, L. N. (2019). Behavioral adaptations to lane keeping systems: Effects of exposure and withdrawal. *Human Factors*, *61*(1), 152–164.

Newell, G. F. (1961). Nonlinear effects in the dynamics of car following. *Operations Research*, *9*(2), 209–229.

Next Generation Simulation (NGSIM) Vehicle Trajectories and Supporting Data. (2016). [Dataset]. Federal Highway Administration. https://catalog.data.gov/dataset/next-generation-simulation-ngsim-vehicle-trajectories-and-supporting-data

Oguchi, T. (2009). Comparative study of car-following models for describing breakdown phenomena at sags through driving simulator experiments. *Proc. of 16th World Congress on ITS, 2009*.

Paxion, J., Galy, E., & Berthelon, C. (2014). Mental workload and driving. *Frontiers in Psychology*, *5*. https://www.frontiersin.org/article/10.3389/fpsyg.2014.01344

Rajamani, R. (2012a). Longitudinal Control for Vehicle Platoons. In R. Rajamani (Ed.), *Vehicle Dynamics and Control* (pp. 171–200). Springer US. https://doi.org/10.1007/978-1-4614-1433-9_7

Rajamani, R. (2012b). Longitudinal Vehicle Dynamics. In R. Rajamani (Ed.), *Vehicle Dynamics and Control* (pp. 87–111). Springer US. https://doi.org/10.1007/978-1-4614-1433-9_4

Rajamani, R., & Zhu, C. (2002). Semi-autonomous adaptive cruise control systems. *IEEE Transactions on Vehicular Technology*, *51*(5), 1186–1192.

Random Forests | SpringerLink. (n.d.). Retrieved July 30, 2022, from https://link.springer.com/article/10.1023/a:1010933404324

Rokach, L. (2019). *Ensemble learning: Pattern classification using ensemble methods*. World Scientific.

Sagi, O., & Rokach, L. (2018). Ensemble learning: A survey. *Wiley Interdisciplinary Reviews: Data Mining and Knowledge Discovery*, *8*(4), e1249.

Saifuzzaman, M., & Zheng, Z. (2014). Incorporating human-factors in car-following models: A review of recent developments and research needs. *Transportation Research Part C: Emerging Technologies*, *48*, 379–403.

Sangster, J., Rakha, H., & Du, J. (2013). Application of naturalistic driving data to modeling of driver car-following behavior. *Transportation Research Record*, *2390*(1), 20–33.

Sewell, M. (2008). Ensemble learning. *RN*, *11*(02), 1–34.

Shi, Y., Li, J., & Li, Z. (2019). *Gradient Boosting With Piece-Wise Linear Regression Trees* (arXiv:1802.05640). arXiv. https://doi.org/10.48550/arXiv.1802.05640

Silva, F. P. da. (2014). Mental Workload, Task Demand and Driving Performance: What Relation? *Procedia - Social and Behavioral Sciences*, *162*, 310–319. https://doi.org/10.1016/j.sbspro.2014.12.212

Simplified Cab miniSim—miniSim. (n.d.). Retrieved November 16, 2022, from https://www.nads-sc.uiowa.edu/minisim/wiki/index.php?title=Simplified_Cab_miniSim#NADS_miniSim.E2.84.A2_Software_and_PC

Stanton, N. A., Young, M., & McCaulder, B. (1997). Drive-by-wire: The case of driver workload and reclaiming control with adaptive cruise control. *Safety Science*, *27*(2–3), 149–159.

Stanton, N. A., & Young, M. S. (2005). Driver behaviour with adaptive cruise control. *Ergonomics*, *48*(10), 1294–1313.

Stapel, J., Mullakkal-Babu, F. A., & Happee, R. (2019). Automated driving reduces perceived workload, but monitoring causes higher cognitive load than manual driving. *Transportation Research Part F: Traffic Psychology and Behaviour*, *60*, 590–605.

Swaroop, D., & Rajagopal, K. R. (2001). A review of constant time headway policy for automatic vehicle following. *ITSC 2001. 2001 IEEE Intelligent Transportation Systems. Proceedings (Cat. No. 01TH8585)*, 65–69.

Tang, T.-Q., Gui, Y., Zhang, J., & Wang, T. (2020). Car-Following model based on deep learning and Markov theory. *Journal of Transportation Engineering, Part A: Systems*, *146*(9), 04020104.

Teoh, E. R. (2020). What's in a name? Drivers' perceptions of the use of five SAE Level 2 driving automation systems. *Journal of Safety Research*, *72*, 145–151. https://doi.org/10.1016/j.jsr.2019.11.005

Treiber, M., Hennecke, A., & Helbing, D. (2000). Congested traffic states in empirical observations and microscopic simulations. *Physical Review E*, *62*(2), 1805.

Treiber, M., & Kesting, A. (2013). Traffic flow dynamics. *Traffic Flow Dynamics: Data, Models and Simulation, Springer-Verlag Berlin Heidelberg*, 983–1000.

Varotto, S. F., Farah, H., Bogenberger, K., van Arem, B., & Hoogendoorn, S. P. (2020). Adaptations in driver behaviour characteristics during control transitions from full-range Adaptive Cruise Control to manual driving: An on-road study. *Transportmetrica A: Transport Science*, *16*(3), 776–806.

Varotto, S. F., Farah, H., Toledo, T., Van Arem, B., & Hoogendoorn, S. P. (2017). Resuming manual control or not?: Modeling choices of control transitions in full-range adaptive cruise control. *Transportation Research Record*, *2622*(1), 38–47.

Varotto, S. F., Farah, H., Toledo, T., van Arem, B., & Hoogendoorn, S. P. (2018). Modelling decisions of control transitions and target speed regulations in full-range Adaptive Cruise Control based on Risk Allostasis Theory. *Transportation Research Part B: Methodological*, *117*, 318–341.

Varotto, S. F., Hoogendoorn, R. G., Van Arem, B., & Hoogendoorn, S. P. (2014). Human factors of automated driving: Predicting the effects of authority transitions on traffic flow efficiency. *Proceedings of the 2nd TRAIL Internal PhD Conference, Delft, The Netherlands, 13 November 2014*.

Wang, X., Jiang, R., Li, L., Lin, Y., Zheng, X., & Wang, F.-Y. (2017). Capturing car-following behaviors by deep learning. *IEEE Transactions on Intelligent Transportation Systems*, *19*(3), 910–920.

Wen, X., Xie, Y., Wu, L., & Jiang, L. (2021). Quantifying and comparing the effects of key risk factors on various types of roadway segment crashes with LightGBM and SHAP. *Accident Analysis & Prevention*, *159*, 106261. https://doi.org/10.1016/j.aap.2021.106261

Wiedemann, R. (1974). *Simulation des Strassenverkehrsflusses.*

Winner, H., Witte, S., Uhler, W., & Lichtenberg, B. (1996). Adaptive cruise control system aspects and development trends. *SAE Transactions*, 1412–1421.

Wu, P., Gao, F., & Li, K. (2019). A vehicle type dependent car-following model based on naturalistic driving study. *Electronics*, *8*(4), 453.

Wu, Y., Kihara, K., Takeda, Y., Sato, T., Akamatsu, M., Kitazaki, S., Nakagawa, K., Yamada, K., Oka, H., & Kameyama, S. (2021). Eye movements predict driver reaction time to takeover request in automated driving: A real-vehicle study. *Transportation Research Part F: Traffic Psychology and Behaviour*, *81*, 355–363.

Wu, Y., Tan, H., Chen, X., & Ran, B. (2019). Memory, attention and prediction: A deep learning architecture for car-following. *Transportmetrica B: Transport Dynamics*, *7*(1), 1553–1571.

Xiao, L., & Gao, F. (2010). A comprehensive review of the development of adaptive cruise control systems. *Vehicle System Dynamics*, *48*(10), 1167–1192.

Xiao, L., Wang, M., & Van Arem, B. (2017). Realistic car-following models for microscopic simulation of adaptive and cooperative adaptive cruise control vehicles. *Transportation Research Record*, *2623*(1), 1–9.

Yan, J., Xu, Y., Cheng, Q., Jiang, S., Wang, Q., Xiao, Y., Ma, C., Yan, J., & Wang, X. (2021). LightGBM: Accelerated genomically designed crop breeding through ensemble learning. *Genome Biology*, *22*, 1–24.

Yang, Y., Wada, K., Oguchi, T., & Iryo-Asano, M. (2015). A Study on Variations of Car-following Behavior at Sag Sections and the Impact of Introducing ACC System. *2015 IEEE 18th International Conference on Intelligent Transportation Systems*, 256–261. https://doi.org/10.1109/ITSC.2015.51

Young, M. S., & Stanton, N. A. (2007). What's skill got to do with it? Vehicle automation and driver mental workload. *Ergonomics*, *50*(8), 1324–1339. https://doi.org/10.1080/00140130701318855

Yu, S., Tang, J., & Xin, Q. (2018). Relative velocity difference model for the car-following theory. *Nonlinear Dynamics*, *91*(3), 1415–1428.

Zhang, D., Chen, X., Wang, J., Wang, Y., & Sun, J. (2021). A comprehensive comparison study of four classical car-following models based on the large-scale naturalistic driving experiment. *Simulation Modelling Practice and Theory*, *113*, 102383.

Zhang, X., Sun, J., Qi, X., & Sun, J. (2019). Simultaneous modeling of car-following and lane-changing behaviors using deep learning. *Transportation Research Part C: Emerging Technologies*, *104*, 287–304. https://doi.org/10.1016/j.trc.2019.05.021

Zhou, J., & Peng, H. (2005). Range policy of adaptive cruise control vehicles for improved flow stability and string stability. *IEEE Transactions on Intelligent Transportation Systems*, *6*(2), 229–237. IEEE Transactions on Intelligent Transportation Systems. https://doi.org/10.1109/TITS.2005.848359

Zhu, M., Wang, X., & Tarko, A. (2018). Modeling car-following behavior on urban expressways in Shanghai: A naturalistic driving study. *Transportation Research Part C: Emerging Technologies*, *93*, 425–445.